Combining colour parameters and geochemical tracers to improve sediment source discrimination in a mining catchment (New Caledonia, South Pacific Islands)

Virginie Sellier[1] • Oldrich Navratil[2] • John Patrick Laceby[3] • Cédric Legout[4] • Michel Allenbach[5] • Irène Lefèvre[1] • Olivier Evrard[1]

[1]Laboratoire des Sciences du Climat et de l'Environnement (LSCE), UMR 8212 (CEA/CNRS/UVSQ-IPSL), Université Paris-Saclay, Gif-sur-Yvette (France)

[2] Laboratoire Environnement Ville Société (EVS), Université Lumière Lyon 2, UMR 5600 (CNRS), Lyon (France)

[3] Alberta Environment and Parks, Calgary, Alberta (Canada)

[4]Institut des Géosciences de l'Environnement (IGE), UMR 5001, Grenoble (France)

[5]LIVE-EA 4243, Université de Nouvelle-Calédonie & LABEX Corail, Nouméa (Nouvelle-Calédonie, France)

Corresponding author: selliervirg@free.fr ; Tel: (33)673910072

Abstract

Over the last century, ~~human activities~~ the intensification of metal mining practices ~~have~~ has induced significant land-cover changes that have accelerated soil erosion processes ~~around the world~~in mining countries. In New Caledonia, a French ~~island~~ archipelago located in the south-west Pacific Ocean, open-cast nickel mining is responsible for soil degradation in almost 10 % of the archipelago's area. This soil degradation results in particular in the increased downstream transfer of sediments in river systems, leading to concerns of siltation of the river systems. In order to reduce this sediment input, ~~has raised many concerns regarding its impact on riverine systems (i.e. hyper-sedimentation, overburden) and the island's ecosystems (i.e. flooding, lagoon siltation, water pollution).~~ quantifying the sediment source contributions from mining activities is required to effectively target the management measures to implement (e.g. types of engineering works, sizing).

Spectroscopy which is a rapid, inexpensive and non-destructive alternative technique to the analysis of geochemical fingerprinting properties may be used to investigate whether eroded sediment is derived from mining sub-catchments or non-mining sub-catchments. ~~A sediment tracing study has been conducted to quantify the contribution of mining versus non-mining sub-catchments in one of the first areas exploited for nickel mining, the Thio River catchment (397 km^2).~~ Sediment deposited during two cyclonic events (i.e. 2015 and 2017) was collected following a tributary design approach in one of the first areas exploited for nickel mining, the Thio River catchment (397 km^2). Source (n= 24) and river sediment (n= 19) samples were analyzed by X-ray fluorescence and spectroscopy in the visible spectra (i.e. 365-735 nm). Four fingerprinting approaches based on (1) colour parameters, (2) geochemical properties, (3) colour parameters coupled with geochemical properties and (4) the entire visible spectrum were tested to discriminate and estimate sediment source contributions.

The results demonstrated that the individual sediment tracing methods based on spectroscopy measurements (i.e. (1) and (4)) did not provide sufficient discrimination between sources. However, the inclusion of colour properties in addition to geochemical parameters (3) provided the highest

discrimination between sources (i.e. 92.6 % of source variance explained). Although with a slightly lower discrimination potential (i.e. 83.1 % of variance explained in sources), the geochemical approach (2) provided similar results to those obtained with the colour coupled with geochemical approach (3). In addition, mixed linear models associated with these two approaches have been experimentally validated with artificial mixture samples. For each of these approaches (2) and (3), the associated fingerprinting properties were used in an optimized mixing model. The predictive performance of the models was validated through tests with artificial mixture samples, i.e. where the proportions of the sources were known beforehand. The results obtained with model (3) showed that mining source tributary contributions strongly dominated the sediments inputs with a mean contribution of 68% ± (SD 25%) for the 2015 flood event and 88% ± (SD 8%) for the 2017 flood event. These results suggest that catchment management should focus on the contributions of mining tributaries to reduce sediment inputs in the river systems. Therefore, the use of these approaches based on geochemical properties individually (2) and coupled to colour parameters (3) could be extended to other mining catchments of New Caledonia but also to other similar nickel mining catchments around the world (e.g. Australia, Brazil, Dominican Republic, Cuba) to estimate sediment source apportionment.

Keywords: Nickel mining • Sediment source fingerprinting • Soil erosion • Modeling

1.Introduction

At the dawn of a fourth industrial revolution, demand for metalliferous minerals continues to increase and impact the world market (Prior et al., 2013;Highley et al., 2004). Currently, open-cast mining generates more than three-quarters of the world's metal ores. However, the extraction of these minerals is associated with deleterious impacts on the environment. In particular, these mines are responsible for the increase in soil erosion and the accelerated transfer of sediment in the river systems. Indeed, bare soil areas generated by mining activities including exploitation sites, prospection areas and access roads significantly increase runoff production (Yellishetty et al., 2013;Dumas et al., 2010;Abel et al., 2000). Moreover, the extraction of mineral ore is accompanied by a sharp production of mining wastes. Until the 1980s, no environmental regulation had been implemented to store this mining waste, and it was dumped directly onto the mountain slopes (Valette-Silver, 1993). Currently, this legacy mining waste provides an active source of sediment as it can progressively be remobilized (Coulthard and Macklin, 2003;James, 2013).

New Caledonia, an island located in the south-western Pacific Ocean and currently the world's sixth-largest producer of nickel, is in particular challenged with the problems of ~~hyper-sedimentation~~ siltation ~~and overburden~~of its river systems. Several studies outline how mining activities, which started in 1875, are generally responsible for these ~~deleterious~~ river morphological changes (Bird et al., 1984;Iltis, 1992;Garcin et al., 2017). ~~The excessive sediment inputs transferred mainly during extreme rainfall events (e.g. cyclones and tropical depressions) lead to the increased occurrence of flooding events in these tropical regions.~~ In this case, excessive inputs of fine and coarse sediment~~s~~ triggered mainly during extreme rainfall events (e.g. cyclones and tropical depressions) have led to the disturbance of the sediment cascade in the river systems. A raising and widening of the riverbed has in particular been observed in the New Caledonian river systems by Garcin et al. (2017), leading to the increased occurrence of flooding events in these tropical regions. Owing to the occurrence of major cyclones in New Caledonia (i.e. on average one cyclone every 2.7 years (Garcin, 2010)), the local population regularly ~~have~~ has to deal with the damage generated by these flood events: ~~(e.g.~~ damage to human settlements, public infrastructure, agricultural land and~~,~~ human casualties~~)~~. Moreover, ~~the island's agricultural and fishing resources are also impacted~~s~~S~~uspended sediment is known to transport large quantities of contaminants in river systems (Kumar and Maiti, 2015;Priadi et al., 2011;Varol, 2011). Hedouin et al. (2007), and more recently Baudrimont et al. (2019), observed high concentrations of trace metals, including Ni and Cr, in marine and freshwater organisms in New Caledonia. These observations raise many questions about the health impact of mining activities on the populations who eat a lot of fish. On a more global level, this anthropogenic activity also threatens the second largest coral reef in the world, listed as a UNESCO World Heritage (Davis and Fox, 2009). In particular, the increased turbidity associated with sediment supply could disrupt coral metabolism (i.e. photosynthetic processes) (Juillot, 2019). These coral reefs provide an exceptional biological diversity and deliver several essential ecosystem services to the local population including fisheries, coastal protection and tourism (Pascal, 2010). The implementation of effective and ~~perennial~~ long-term sediment control measures on mining sites (e.g. sediment retention basin, revegetation) is therefore required to reduce sediment inputs into the lagoon. At this end, quantifying the sediment source contributions from mining activities

~~Erosion generated by open-cast nickel mining (i.e. mining bare soil, mining roads, mining prospection and mining waste) do not provide the only sediment source in New Caledonia's mining catchments. The use of fires to clear landscapes conducted by the local population for farming, pasture and hunting increase the area of bare soils (Dumas et al., 2010). Soils that are left uncovered by vegetation are more sensitive to erosion and they may be exposed to shallow landsliding (Blake et al., 2009;Smith et al., 2011). Moreover, several invasive species such as deers or wild pigs also threaten soil stability through trampling and overgrazing .~~

~~The contribution of mining tributaries (i.e. draining mining areas) and non-mining tributaries (i.e. draining areas without mining activities) to sediment transiting catchments in New Caledonia therefore~~

~~needs to be discriminated. This discrimination has particularly~~ becomes particularly important as the mining industries are subject to the "polluter pays" principle applied since 1975, i.e. the obligation to fund remediation according to the extent of the damage generated by mining activity on the environment (Clarke and David, 2010). ~~There is therefore a real social, environmental and financial challenge in discriminating between sediment sources generated by mining activities and other potential sediment sources.~~ Discriminating between sediment sources generated by mining activities and other potential sediment sources is therefore a real social, environmental, political and financial challenge in New Caledonia.

Indeed, other sediment sources that are not associated with mining activities as deforestation, farming, pasture may contribute to sediment inputs in river systems. The use of fires to clear landscapes also increases the area of bare soils (Dumas et al., 2010). Moreover, several invasive species such as deers or wild pigs threaten soil stability through trampling and overgrazing (Shellberg et al., 2010). Soils that are left uncovered with vegetation are more sensitive to erosion and they may be exposed to landslides (Blake et al., 2009;Smith et al., 2011).

Sediment fingerprinting techniques have been developed since the 1970s to determine the spatial origin of sediment sources and quantify their contributions (Klages and Hsieh, 1975;Walling et al., 1979;Brown, 1985). These techniques are based on the analysis of multiple conservative properties both in the sediments and their potential sources. The properties must necessarily be conservative, i.e. the ranges of variation of these properties in the river material have to be predictable based on those measured in the sediment sources. The ability of one or more of these properties to discriminate between sources then allows to estimate the relative contribution of each source through the use of a mixing model (Collins and Walling, 2002). Fallout radionuclides (Wallbrink, 2004;Evrard et al., 2015;Evrard et al., 2020), geochemical (Laceby and Olley, 2015;Batista et al., 2018) and mineral properties (Gruszowski et al., 2003;Motha et al., 2004) are the most frequently used tracers to quantify sediment source contributions. The use of fallout radionuclides and geochemical properties as potential tracers was investigated to quantify the sources of suspended sediment in the Thio River catchment (397 km²), one of the first catchments in New Caledonia to be mined for nickel. Fallout radionuclides proved to be unsuitable (i.e. non-discriminatory) while g~~G~~eochemical properties provided promising results, i.e. 83.1 % of variance explained in sources ~~while the fallout radionuclides proved to be unsuitable (i.e. non-discriminatory)~~ (Sellier et al., 2019). The discrimination offered by geochemical properties was particularly explained by the differences in geochemical composition outlined by Sevin (2014) between the two dominant lithologies found in the archipelago: volcano-sedimentary formations covering two thirds of the archipelago and peridotite massifs covering the remaining third where mining activities are located. Mining erosion dominates 95% of eroded areas identified -on peridotite massifs of the Thio River catchment according to the remote sensing study carried out by Garcin et al. (2017). As a result, using geochemical properties is effective to indirectly quantify the sediment contributions from mining activities and from areas devoid of mining activities. In this case, K provides -a straightforward tracer to discriminate the sediment sources (Sellier et al., 2019). Indeed, volcano-sedimentary rock formations naturally contain high K elemental contents whereas peridotite massifs are depleted in this element in New Caledonia (Sevin, 2014). Although these initial study results were very promising~~However~~, other less expensive, faster and possibly more efficient techniques than the more conventional methods previously tested could be envisaged. For example, spectroscopy in the mid-infrared (MIR) (Poulenard et al., 2009), the visible near-infrared (VNIR) and the shortwave-infrared (SWIR) (Brosinsky et al., 2014) ~~regions of~~ spectra have been used to quantify the sediment source contributions. ~~It~~ Spectroscopy is also non-destructive and requires low quantities of sample material. Spectroscopy could therefore meet both the need for a simple, inexpensive, ~~and~~ fast and portable ~~rapid~~ sediment tracing method in a context where flood events are frequent. This analysis technique could also be more easily transferred to local populations so that they can carry out long-term environmental monitoring of sedimentary contributions themselves.

Moreover, the geological specificity of the archipelago provides a strong contrast in terms of soil colours observed either on the peridotite massifs or on the volcano-sedimentary formation rocks and by extension, on the eroded sediments derived from these soils. ~~New Caledonia has a specific geological feature which is at the origin of its mineral wealth: one third of its surface area is covered with peridotite massifs.~~ On the one hand, ~~T~~the weathering of ~~these rocks~~peridotite massifs naturally enriched in Fe and transition metals such as Mn, Ni, Cr and Co results in the formation ~~of Ni- and Fe-rich smectite, serpentine, goethite and hematite~~ of laterite profile composed of peridotites, saprolites, yellow laterites and red laterites (from the bottom to the top). ~~The oxidized minerals (i.e. goethite and hematite)~~Hypermagnesian and ferrallitic ferritic soils that are rich in goethite and hematite and that formed on the surface provide a particularly reddish-orange colour to sediment derived from these exploited soils (i.e. mining sources, Figure 1) (Quantin et al., 1997;Trescases, 1973). On the other hand, the weathering of volcano-sedimentary formation rocks generates the formation of altered horizons rich in goethite and clay horizons rich in kaolinite (from the bottom to the top) (Denis, 1988). The eroded sediment derived from fersialitic soils formed on the surface is characterized by a yellow-grey colour (Figure 1). ~~mining sources that distinguishes them from non-mining sources, which tend to be grey in colour.~~ The differences made visually between the two sources further encourage the analysis of sources by spectroscopy and especially spectroscopy in the visible region of the spectrum (i.e. 365-735 nm). In particular, the colorimetric parameters derived from the visible spectrum have been shown to be effective in discriminating sediment sources. Their discrimination power has been tested both individually (Evrard et al., 2019;Martínez-Carreras et al., 2010;Uber et al., 2019) and in combination with other tracers (e.g. geochemical properties (Tiecher et al., 2015)) according to the conventional fingerprinting approach (i.e. statistical analysis and use of a mixing model) (Collins et al., 1996). A more alternative approach based on the entire visible spectrum with the partial least square regression (PLSR) models has also been developed to trace origin of sediment sources in the literature (Legout et al., 2013;Tiecher et al., 2015).

Figure 1 Photographs of river material deposited on the channel banks of a mining tributary (left) and a non-mining tributary (right) in the Thio River catchment

As part of this study, four sediment fingerprinting methods based on (1) colour parameters, (2) geochemical properties, (3) colour parameters coupled with geochemical properties and (4) PLSR models based on the whole visible spectrum were tested in the Thio River catchment. A tributary design approach was implemented to trace the origin of sediments, i.e. sediment samples collected on different tributaries were used as potential sources of the river sediment collected further downstream on the Thio River (Laceby et al., 2017). Source (n=24) and river sediment (n=19) samples were collected ~~following a tributary design approach~~ and analyzed by X-ray fluorescence and spectroscopy in the visible spectra (i.e. 365-735 nm). For each of these sediment fingerprinting methods, the associated potential tracing properties were used in an optimized mixing model. ~~The performance of each method to estimate sediment source contributions was evaluated~~Tests with artificial mixture samples, i.e. where the proportions of the sources were known beforehand were carried out to evaluate the predictive performance of each model in order to select the best technique to be applied in the Thio River catchment and possibly in other mining catchments of New Caledonia.

~~On a wider scale, the tracers retained in this study could be considered as potential sedimentary tracers to estimate sediment source apportionment in other similar nickel mining catchments around the world (e.g. Australia, Brazil, Dominican Republic, Cuba).~~

2.Materials and methods

2.1 Study area

Located in the southwestern Pacific Ocean, New Caledonia (18 500 km²) is made up of several islands, the largest of which is *La Grande Terre* (17 000 km²). The Thio River catchment (397 km²) is located on the east coast of this island (Figure ~~1~~2-a). It has a mountainous relief, with an average altitude of 416 m above sea level (i.e. minimum: 0 m, maximum: 1392 m, Figure ~~1~~2-a) and an average slope of 45%. Two dominant lithologies are present in the catchment: volcano-sedimentary formations mainly located on the western part of the catchment and peridotite massifs concentrated in the eastern part of the catchment. Cherts (22 %), sandstone (9 %), a mix of basalt, dolerite and gabbro (6 %), polymetamorphic rocks (6 %) mainly constitute volcano-sedimentary formations whereas peridotite massifs are composed of laterites (18 %), peridotites (17 %), serpentines (10 %) and hazburgites (1 %) (Garcin et al., 2017) (Figure 1-b). The rock formation of these lithologies plays a key role in determining their degree of soil erodibility. In this case, Dumas (2010) described that volcano-sedimentary formations are less sensitive to soil erosion than peridotite massifs. Indeed, rocks from volcano-sedimentary formations such as basalts and cherts provide a certain resistance to erosion whereas laterites at the top of the profile are extremely sensitive to erosion processes, which explains why most forms of concentrated erosion (e.g. gullies, rills) and mass movements are mainly observed on peridotite massifs (Figure 3). However, the permanent vegetation covering 96% of the Thio River catchment surface offers a relative protection against soil erosion across the catchment. ~~The Thio River catchment is covered on 96% of its surface by permanent vegetation.~~ Peridotite massifs naturally enriched in heavy metals have a low soil fertility, which explains why farming or pasture activities are not implemented on these soils (Quantin et al., 1997). Peridotite massifs have been exploited exclusively for their nickel resources since 1875. According to the mining registry, active and abandoned mining sites and exploration cover 21 % of the catchment area (Figure ~~1~~2-c).

The Thio River catchment is subject to a tropical climate characterized by the alternation of a hot wet season (November-April; mean temperature of 27 °C) and a cooler dry season (May-October; mean temperature of 20 °C). The mean annual rainfall in the Thio River catchment is 1620 mm despite strong seasonal fluctuations with the highest levels of precipitation recorded during the cyclonic season between January and March (700 mm, 1981-2008; Alric (2009)). Although they only occur on average once every 2.7 years, cyclones or tropical depressions may supply more than 20 % of the annual rainfall in only one day according to local meteorological records (Météo France).

Twelve major tributaries flow into the main stem of the Thio River (28 km long) (Figure 12-b). Ninety-two percent of the river channel length are characterized with slopes lower than 5 %. According to Surell's classification (1841), the Thio River can be considered as torrential except in its estuarine section. In addition, the longitudinal connectivity is exacerbated by In addition, the extensive 8km² of bare soil surfaces associated with past mining activities (~10 sites),), ongoing mining operations (e.g. 2 sites: Thio Plateau, Camps des Sapins) and the occurrence of 6 km² of mining roads. Bare soil areas increase soil erosion processes on peridotites massifs, which once initiated, are difficult to contain (Figure3). Heavy rainfall and the associated runoff exacerbate exacerbate runoff production as they contribute to increased river network connectivity (Alric, 2009). This generates extensive erosion processes that are evident across the entire Thio catchment with the widespread occurrence of rills, gullies, landslides and channel bank erosion (Danloux and Laganier, 1991), thus contributing to connect the sediment sources to the tributaries and consequently to the main river (Figure 3). For low intensity floods (i.e. <200 $m^3.s^{-1}$), a strong remobilization of sediments in New Caledonian river systems has been observed (Allenbach et al., 2020), thereby indicating that a lateral connectivity occurs in the Thio River catchment through the occurrence of channel bank erosion.

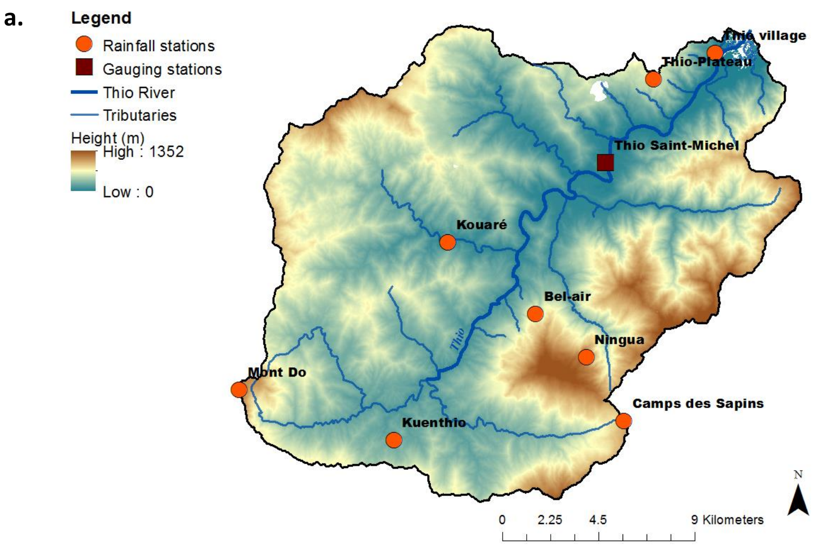

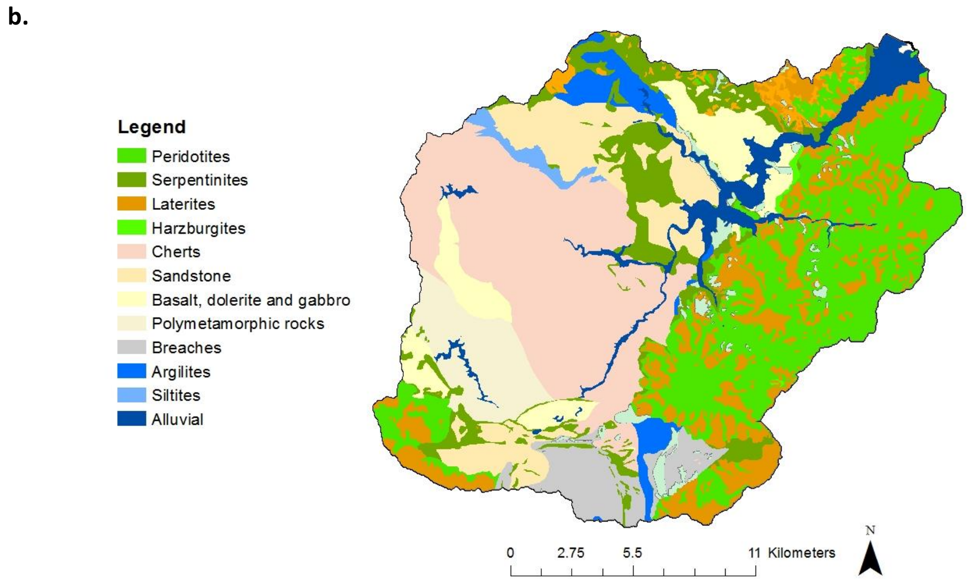

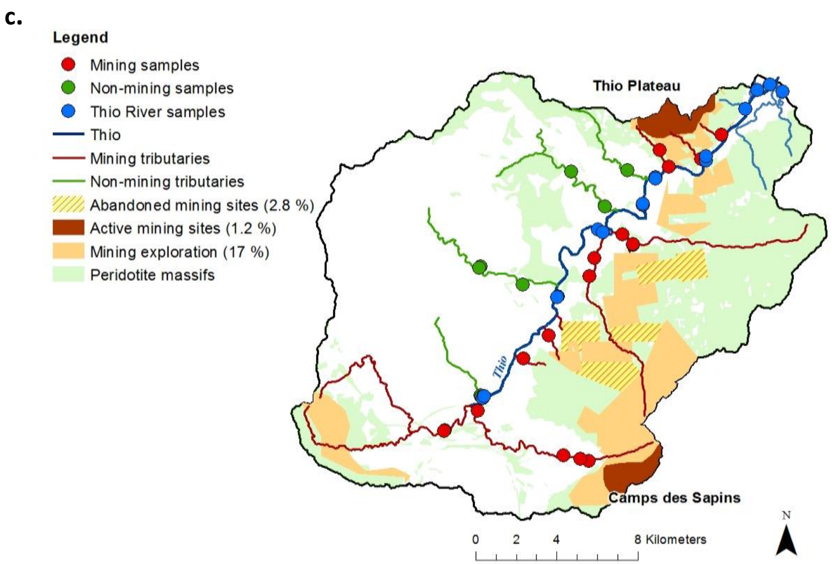

Figure ~~3~~ 2 Location of the rainfall and river monitoring stations (a), main lithologies (b) and location of the sediment samples collected along with tributary source classifications (c) conducted in the Thio River catchment, New Caledonia

Figure 3 Photographs of concentrated erosion and mass movement processes observed on peridotite massifs of the Thio River catchment

2.2 Hydro-sedimentary monitoring

Three rainfall stations (Thio Plateau, Thio village, Camps des Sapins; Figure ~~1~~2-b) are operated by Météo France and five others are managed by the DAVAR (Direction des Affaires Vétérinaires Alimentaires et Rurales; i.e. Kouaré, Bel-Air, Ningua, Kuenthio, Mont Do), with daily records available since 1952 for some stations (e.g. Thio village). Daily discharge has been monitored at a river gauging station located on the main stem of the Thio River (at Saint-Michel) since 1981 by the DAVAR (Figure 1-a).

2.3 Sources and river sediment sampling

In this study, two extreme events were investigated: Cyclone Murcia on February 25, 2015 and Cyclone Cook on April 10, 2017. These cyclones respectively contributed to 7 % of annual rainfall in 2015 and 25 % in 2017~~,~~. T~~t~~hey generated floods with a return period of 10 years (i.e. 3500 $m^3.s^{-1}$). To trace the origin of sediment, lag deposits were collected as an alternative of suspended sediment sampling on channel bars of mining tributaries (n= 16), non-mining tributaries (n= 8) and the Thio River (n= 19) according to the tributary design approach recommended by Laceby et al. (2017) (Figure ~~1~~2-c). They were sampled after the two major floods ~~(~10 year return period):~~ generated by ~~(1) the tropical depression of~~Cyclone Murcia ~~February 25, 2015~~ (n= 31) and ~~(2)~~ Cyclone Cook ~~on April 10, 2017,~~ (n= 12). These two sample sets were respectively sampled between April 30 and May 5, 2015 and between May 16 and 17, 2017. At each sampling site, five to ten subsamples of fine sediment were collected depending on the amount of observed sedimentary material. They were sampled across a 10 m^2 surface with a plastic trowel at exposed subaerial sites free of vegetation on channel bars. The subsamples were composited into one sample representative of the fine sediment deposited on the channel bars. The samples were oven-dried at 40°C for ~48 hours ~~and sieved to 63 µm~~. Particle size selectivity may occur during the erosion, transport and deposition processes inducing an overall finer particle size distribution in the river material compared to the sources. This selectivity can lead to a non-conservation of the fingerprinting properties. For example, certain properties are preferentially contained in a given particle size fraction which can create a relative enrichment or conversely a relative depletion of these properties in the river material according to the particle size fraction analyzed. In order to avoid this particle size effect, river sediment and source samples were sieved to 63 µm, which is the most commonly used fraction in sediment tracing research (Owens and Walling, 2002;Navratil et al., 2012).

2.4 Preparation of artificial mixture samples

Equal quantities of all mining ~~source~~ tributary samples (0.4g for each sample, n= 16) were mixed together to create a composite sample which would have an overall geochemical and colour signature of the mining sources in the Thio River catchment (i.e. 'Mining source' pole). The same process was carried out with non-mining ~~source~~ tributary samples(0.4g for each sample, n= 8, 'Non-mining source' pole). 'Mining source' and 'Non-mining source' pole samples were then mixed in known proportions to create artificial mixture samples (n= 21, 0-100 % with a 5 % step, Table 1).

Table 1 Proportions of mining and non-mining sources (%) in artificial mixture samples (M_i). *M6 was withdrawn from this study because an error occurred at the time of its completion (~~out of the study~~ not consider in the study).*

M_i	Proportions of 'mining source' pole (%)	Proportions of 'non-mining source' pole (%)
M1	0	100
M2	5	95
M3	10	90
M4	15	85
M5	20	80
M6	*25* ~~(out of the study)~~ (*not consider in the study*)	*75* ~~(out of the study)~~ (*not consider in the study*)
M7	30	70
M8	35	65
M9	40	60
M10	45	55
M11	50	50
M12	55	45
M13	60	40
M14	65	35
M15	70	30
M16	75	25
M17	80	20
M18	85	15
M19	90	10
M20	95	5
M21	100	0

2.5 Source, river sediment and artificial mixture sample analyses

Spectroscopy measurement in the visible were carried out with a~~A~~ portable diffuse reflectance spectrophotometer (Konica Minolta 2600d) at the Institut des Géosciences de l'Environnement (IGE, Grenoble, France). To this end, between 0.1 g and 4 g of Thio River sediment (n= 19), source (n= 16) and artificial mixture samples (n= 20) were stored in 60 mL polystyrene tubes. In order to perform the analyses, the spectrophotometer was installed on a flat surface with the measuring window facing upwards. The tubes were then placed on the 3-mm radius circle measuring cell. Because of the rather small measuring area and to take into account the possible heterogeneity within the samples, three measurements were carried out on river sediment and sources samples. For artificial mixture samples, the experimenter who conducted the analyses performed four measurements. Spectral reflectances were measured between 365 nm and 735 nm with a 10-nm resolution. Several parameters were applied for each measurement: D65 illuminant, 10° angle observer and specular component excluded. Raw data collected corresponds to the spectral reflectance percentage for each of the 39-wavelength classes. From these raw data, 15 variables of various colorimetry models were derived. Among these components, XYZ tri-stimulus values were calculated based on the colour-matching functions defined by the International Commission on Illumination (CIE 1931). The standardized tri-stimuli were then converted into CIELab and CIELu'v' cartesian coordinate systems using the equations provided by CIE (1976) and then into CIELch, CIEL*a*b* cartesian coordinate systems using the equations provided by CIE (1994) (Rossel et al., 2006). First Derivative reflectance of the Visible Spectra (FDVS) of each sample was also derived from the initial reflectance spectrum. According to Tiecher et al. (2015), the use of FDVS avoids differences in baseline positions and allows to get rid of the small differences due to uncontrolled sources of variation, as sample packaging. A zero and a white calibration were performed before each set of measurements. In addition, and in order to evaluate a potential drift of the device's signal, control measurements were carried with red, green, yellow panels and three contrasted sediment samples before and after each set of measurements.

~~was used to measure the spectra in the visible (365-735 nm with a 10-nm resolution, 39-wavelength class) on Thio River sediment (n= 19), tributary source (n= 16) and artificial mixture samples (n= 20). Sample quantities between 0.1 g and 4 g were stored in 60 mL polystyrene tubes and analyzed at the Institut des Géosciences de l'Environnement (IGE, Grenoble, France). Because of the rather small measuring area (i.e. 3-mm radius circle), and to take into account the possible heterogeneity within the samples, three measurements were carried out on river sediment and~~

sources samples. For artificial mixture samples, the experimenter who conducted the analyses carried out four measurements. Several parameters (i.e. D65 illuminant, 10° angle observer and specular component excluded) were applied for each measurement. Raw data collected corresponds to the spectral reflectance percentage for each of the 39-wavelength class. From these raw data, 15 variables of various colorimetry models were derived. Among these components, XYZ tri-stimulus values were calculated based on the colour-matching functions defined by the International Commission on Illumination (CIE 1931). The standardized tri-stimuli were then converted into CIELab and CIELu'v' cartesian coordinate systems using the equations provided by CIE (1976) and then into CIELch, CIEL*a*b* cartesian coordinate systems using the equations provided by CIE (1994) (Rossel et al., 2006). First Derivative reflectance of the Visible Spectra (FDVS) of each sample was also derived from the initial reflectance spectrum. According to Tiecher et al. (2015), the use of FDVS avoids differences in baseline positions and to get rid of the small differences due to uncontrolled sources of variation, as sample packaging.

Measurements of 11 geochemical elements (i.e. Mg, Al, Si , K, Ca, Ti, Cr, Mn, Fe, Ni and Zn) on the samples were conducted by pre-calibrated energy dispersive X-ray fluorescence spectrometry (Epsilon 3, Malvern PANalytical) with certified reference samples including Internal Atomic Energy Agency (IAEA) standards. Correlations between the determined and the standard elemental contents were comprised between 0.90 and 0.99. The associated mean relative error was 9 % (SD 8 %). (r^2 = 0.90-0.99, mean relative error: 9% ,SD 8 %, minimum: 1%, maximum: 23%). Between 0.2 and 0.5 g of the samples were packed in small mass holder (SMH) cells with an air double X-ray Mylar film and analyzed at the Laboratoire des Sciences du Climat et de l'Environnement (LSCE, Gif-sur-Yvette, France). Samples were irradiated with a primary beam generated by an Rh anode X-ray tube emitting electromagnetic waves between 100eV and 1MeV with a maximum power, typical current and voltage fixed to 15 W, 3mA and 50 kV respetively. The associated Si-drift detector had a Be window thickness of 8 µm and recorded the sample spectrum in a 2D optical geometry configuration. X-ray intensities were converted into concentrations using the Epsilon 3 software program through the application of the fundamental parameters method.

2.6 Statistical analysis and sediment tracing

2.6.1.Conventional mixing model

In general, the sediment source fingerprinting approach is composed of four main steps: (1) range test, (2) the Mann-Whitney U test, (3) a stepwise discriminant function analysis and (4) a mixing model (Collins et al., 1996;Laceby and Olley, 2015). For the range test, all variables exhibiting values in the river sediment samples that were outside of the range found in the potential sources (i.e. between the minimum and maximum values found in source samples) were excluded from the analysis. It is important to restrict the tracing parameters to those that show a conservative behavior to avoid incorrect source prediction and consequently inaccurate estimations of source contributions (Sherriff et al., 2015). Thereafter, the Mann-Whitney U test (α= 0.05, p-value <0.01) was performed to evaluate whether remaining variables could discriminate the source samples. A stepwise discriminant function analysis (DFA) was independently run on three set of potential tracing properties: (1) colour parameters (i.e. 'colour'), (2) geochemical properties (i.e. 'geochemistry') and (3) colour parameters and geochemical properties (i.e. 'colour + geochemistry'). For the last set, the raw values of the variables were normalized in order to make them comparable. Indeed, several colour parameters were within an order of magnitude of around 0.01 whereas for the geochemical parameters the difference was around 10^6 mg kg^{-1} which resulted in a poorly conditioned matrix for the DFA.

The following calculation was therefore applied on the variable values to normalize them: x_i – x_{min}/ x_{max} - x_{min} where xi was value found in source sample (i), x_{min} and x_{max} were respectively the minimum and maximum values found in the source samples. The DFA was carried out to select the optimal number of potential tracers to discriminate the sources for each modelling approach with the optimal number of potential tracers which must provide the lowest Wilks' lambda value from analysis of variance. Indeed, the closer the Wilks' lambda value is to 1, the lower the variability within the sources compared to the total variability. The DFA was performed in the backward mode with a $p > 0.01$ used to select a tracer and $p < 0.01$ used to remove a tracer. The *Statistica* software was used to carry out the DFA because it has the advantage of automatically identifying and eliminating collinear variables.

Finally, a classical solver-based mixing model was used to model the source contributions from the mining and non-mining tributaries to target sediment through simultaneously minimizing the mixing model difference (MMD) (Evrard et al., 2019):

$$MMD = \sum_{i=1}^{n} ((C_i - (A_i x + B_i(1-x))/C_i) \quad Equation\ 1$$

where n is the number of parameters in the model chosen by the selection process (i.e. steps 1, 2, 3); C_i is the Thio River sediment sample parameter (i); x and (1-x) were respectively the contributions of source A and B (i.e. mining and non-mining tributaries); A_i is the mean of parameter (i) in source A and B_i is the mean of parameter (i) in source B. The proportional contribution from each source (x) was modelled by solving Equation 1 with the Solver Function in Microsoft Excel with x being between 0 and 1 and the sum of source contributions (i.e. x and 1-x) equaling 1. The GRG Non-Linear solving method was used with automatic scaling in Solver, ignoring integer constraints, with a maximum run time of 5000 and allowing for 2500 iterations. ~~A multi-start population size of 2500 was used along with the same random seed for each of the model runs while requiring bounds on the variables.~~ For each of the 2500 iterations, the values of the variables were determined randomly with respect to their initially fixed ranges of values. A constraint precision and convergence of $1.0\ 10^{-6}$ were selected for each of the model runs. To test the reliability of the 'colour', 'geochemistry' and 'colour + geochemistry' models, these latter were tested on artificial mixture samples.

2.6.2.FDVS- PLSR model

FDVS-PLSR models were built following the methodology described in Poulenard et al. (2012). The first step consisted in applying a principal component analysis (PCA) to evaluate the overall variability between FDVS (i.e. ~~38~~ 38-wavelength class) of source samples. Subsequently, a discriminant analysis (DA) was conducted based on the PCA scores. The purpose of this analysis was to compare the Mahalanobis distance between sources samples and to determine if FDVS of source samples could discriminate the sources. Relationships between FDVS (x variate) and the corresponding weight contribution of the sediment source data sets (y variate) were analyzed using PLSR. The PLSR models were carried out based on the component set providing the lowest predictive error (PRESS, option on XLStat software). Two independent PLSR models were built to estimate the two sediment source contributions. As the artificial mixtures were measured four times by spectroscopy, 84 FDVS of artificial mixture samples were generated including 50 values that were randomly selected to build the models (training set (ST)) and 34 to validate the models (validation set (SV)). The SV:ST ratio used was approximately 1:2, which is in agreement with recommendations provided in the literature (Daszykowski et al., 2002). To evaluate the performance of PLSR models, several indicators such as coefficient of linear regression (r^2), root mean square error of calibration (RMSEC) and root mean square error of prediction (RMSEP) values were calculated. Unlike the conventional fingerprinting approach, the estimated contributions of sources were not limited to be in the range of 0 % and 100 %. In a similar way, the sum of source contributions was not constrained to be equal to 100 %. As a result, another way to control the reliability of predictions was to sum the prediction proportions of both models (Legout et al., 2013). FDVS of river sediment samples were then introduced into these PLSR models to estimate the contribution of sediment sources.

3.Results

3.1 Source description

The ranges of values of all colour parameters measured in the Thio River sediment samples systematically plotted within the range of values observed in the two potential sources (i.e. mining and non-mining tributaries; Figure ~~2~~ 4 and Table 2). The range test results confirmed the conservative character of these parameters. For geochemical properties, elemental concentrations measured in the river sediment also plotted within the range of concentrations found in sources (Sellier et al., 2019). ~~According to the range test results~~In similar way, the range tests applied on geochemical properties showed that~~,~~ all these properties were also ~~determined to be~~ conservative.

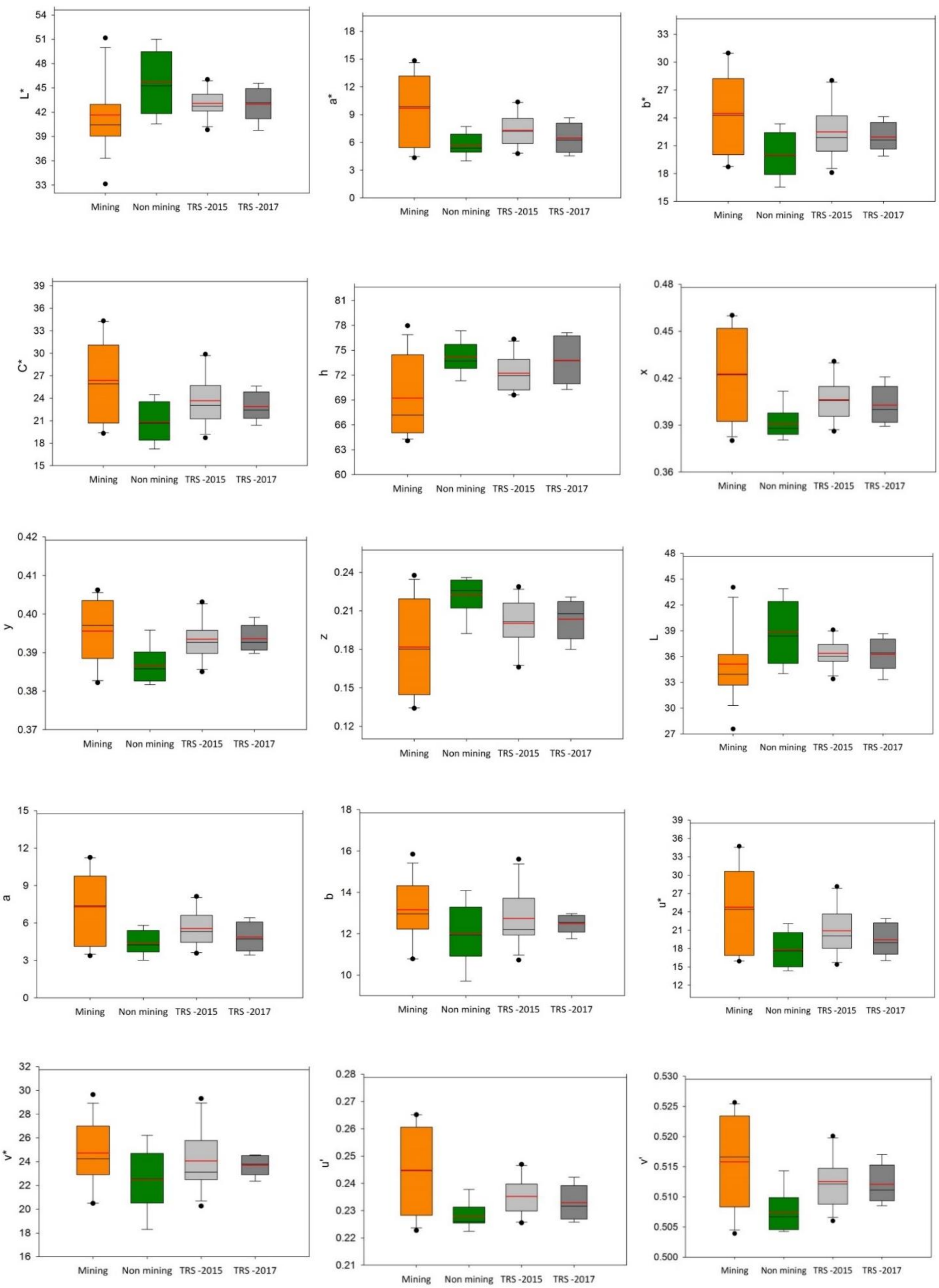

Figure 4 Box-plots of colour parameter values in the <63 µm fraction of sediment collected on the mining tributaries (Mining), non-mining tributaries (Non-mining) and the main Thio River (Thio River sediment (TRS)-flood events of 2015 and 2017). The box indicates the location of the first and third quartiles; the black line indicates the median value; the red line indicates the mean value

Table 2 Mean values of ~~Geochemical~~ geochemical element contents and colour parameters ~~values~~ in the <63 µm fraction of sediment sources and Thio River sediment (SD: standard deviation); results of Mann-Whitney U test and individual DA used to identify the potential tracers to differentiate sources supplying sediment to the Thio River

Fingerprinting property	Mann-Whitney U test		DA- correctly classified samples (%)	Mean ± SD			
	U-value	p-value		Mining tributaries (n= 16)	Non-mining tributaries (n= 8)	Thio River sediment 2015 (n= 11)	Thio River sediment 2017 (n= 8)
Geochemical tracers							
Al *(g kg^{-1})*	8	0.000	87.5	21 ± 21	67 ± 8	43 ± 15	29 ± 6
Ca *(mg kg^{-1})*	21	0.007	62.5	3731 ± 470	9286 ± 5194	5281 ± 1201	3945 ± 666
Cr *(mg kg^{-1})*	124	< 0.0001	83.3	7480 ± 4606	706 ± 967	4359 ± 2185	5715 ± 1786
Fe *(g kg^{-1})*	121	0.000	91.6	144 ± 70	62 ± 24	43 ± 15	29 ± 6
K *(mg kg^{-1})*	2	< 0.0001	95.8	1657 ± 2160	14019 ± 3702	5944 ± 3294	3750 ± 974
Mg *(g kg^{-1})*	119	0.000	83.3	99 ± 59	16 ±13	88 ± 33	117 ± 21
Mn *(mg kg^{-1})*	108	0.006	83.3	2531 ± 1317	1439 ± 606	2068 ± 667	1786 ± 516
Ni *(mg kg^{-1})*	125	< 0.0001	91.6	6576 ± 5075	358 ± 339	4218 ± 1938	4341 ± 1239
Si *(g kg^{-1})*	6	< 0.0001	91.6	178 ± 42	254 ± 28	221 ± 15	204 ± 7
Ti *(mg kg^{-1})*	13	0.001	87.5	1409 ± 2077	5446 ± 835	2771 ± 1197	1663 ± 457
Zn *(mg kg^{-1})*	68	0.834	-	146 ± 47	125 ± 4	134 ± 17	125 ± 8
Colour parameters							
L*	24	0.013	-	41.6 ± 4.6	45.7 ± 3.9	43.1 ± 1.7	43.0 ± 2.0
a*	104	0.013	-	9.7 ± 3.8	5.7 ± 1.2	7.3 ± 1.9	6.5 ± 1.7
b*	106	0.009	70.8	24.5 ± 4.5	20.0 ± 2.5	22.5 ± 3.0	21.9 ± 1.6
C*	108	0.006	66.6	26.4 ± 5.5	20.8 ± 2.7	23.7 ± 3.5	22.9 ± 2.0
h	26	0.019	-	69.2 ± 4.8	74.2 ± 1.9	72.2 ± 2.2	73.8 ± 2.9
x	107	0.007	75	0.42 ± 0.03	0.39 ± 0.01	0.41 ± 0.01	0.40 ± 0.01
y	111	0.003	79.2	0.396 ± 0.008	0.387 ± 0.005	0.393 ± 0.005	0.394 ± 0.004
z	19	0.005	75	0.18 ± 0.04	0.22 ± 0.01	0.20 ± 0.02	0.20 ± 0.02
L	27	0.013	-	35.1 ± 4.2	38.9 ± 3.7	36.4 ± 1.6	36.3 ± 1.9
a	103	0.016	-	7.3 ± 2.9	4.4 ± 1.0	5.6 ± 1.5	4.9 ± 1.2
b	91	0.106	-	13.1 ± 1.5	12.0 ± 1.5	12.7 ± 1.4	12.5 ± 0.4
u*	101	0.023	-	24.8 ± 6.9	17.8 ± 2.8	20.9 ± 4.0	19.4 ± 2.7
v*	93	0.081	-	24.7 ± 2.8	22.5 ± 2.7	24.1 ± 2.6	23.7 ± 0.8
u’	105	0.011	-	0.245 ± 0.016	0.228± 0.005	0.235 ± 0.007	0.233 ± 0.007
v’	111	0.003	79.2	0.516 ± 0.008	0.507 ± 0.004	0.513 ± 0.004	0.512 ± 0.003

3.2 Selection of parameters/properties for modelling

1.2.1. ‘Colour’ model

According to the Mann-Whitney U test results, six colour parameters (*i.e.* b*, C*, x, y, z, v’) provided significant discrimination between the two sediment sources (*i.e.* p-value < 0.01, Table 2). The backward DFA selected only v’ as the optimal tracer of mining and non-mining source sediments (Figure ~~2~~4, Table 3). Although this parameter correctly classified 79.2 % of sources, the high Wilk’s lambda value obtained (i.e. 0.7209, Table 3) induced that only 27.9 % of variance was explained by v’. The low Mahalanobis distance value obtained (i.e. 1.6) confirmed that sediment sources were not well separated. Accordingly, and owing to the high error percentage of the source discrimination provided by this approach (i.e. 72.1 %), source contributions were not modeled with the ‘colour’ model.

1.2.2. ‘Geochemistry’ model

When considering the two potential sediment sources, all geochemical properties (except Zn) were selected as potentially discriminant by the Mann-Whitney U test (i.e. p-value < 0.01, Table 2). Among the 10 potential tracers, K was selected by the backward DFA to model sediment source contributions from mining and non-mining tributaries with 95.3 % of sources correctly classified and 83.1 % of variance explained by K. This percentage of variance explained was deduced from the final Wilk’s lambda value obtained (i.e. 0.1691). Moreover, the Mahalanobis distance value showed that the sediment sources were well separated from each other with a significant distance of 20.3 (Table 3) (Sellier et al., 2019).

1.2.3. ‘Colour + geochemistry’ model

When combining colour parameters and geochemical properties, the DFA selected five optimal tracers (i.e. K, Ca, Ti, b*, C*) able to correctly classify 100 % of the sources. A significant improvement in the source discrimination was observed with the lowest Wilk’s lambda value obtained (i.e. 0.0734) and the highest percentage of variance explained (i.e. 92.6 %). Moreover, the Mahalanobis distance value obtained (i.e. 52.1) was more than 2.5 times higher than that estimated with the 'geochemistry' model (Table 3), thus resulting in a better separation between sediment sources than the previous approach (i.e. 'geochemistry')

Table 3 Results of DFA used to identify the optimum tracer combination to differentiate sources supplying sediment to the Thio River

Fingerprint property selected	Wilks'Lambda	Variance explained by the variables (%)	Squared Mahalanobis distance	Correctly classified samples (%)
'Colour'				
v'	0.7209	27.9	1.6	79.2
'Geochemistry'				
K	0.1691	83.1	20.3	95.3
'Colour + Geochemistry'				
K, Ca, Ti, b*, C*	0.0734	92.6	52.1	100

3.3 Assessment of model performance on artificial mixture samples

Prior to applying mixing models to river sediments, preliminary tests were conducted to control the validity of the models (i.e. 'geochemistry' and 'colour + geochemistry') and the associated estimations of source contribution errors. When applying these models on the artificial mixture samples, actual and predicted proportions were well correlated for both models (i.e. r^2= 0.99 and r^2= 0.98 respectively for 'geochemistry' and 'colour + geochemistry' models, SD_{max} = 3 %) (Figure ~~3~~5).

However, the 'geochemistry' model described in Figure ~~3~~5-a showed that the contributions of mining tributaries were overestimated. With 100 % of actual mining contributions, 100 % of mining contribution was predicted by the model. However, instead of 0 % of actual mining contributions, a mining contribution of 15.5% was predicted by the model. It means that the more the estimated mining source contributions tends towards 0 %, the greater the associated overestimation (i.e. maximum 15.5 %) (Figure ~~3~~5-a). The 'colour + geochemistry' model also provided a slight overestimation of the contribution of mining tributaries (i.e. 7 % intercept of the regression line, Figure ~~3~~5-b). Given the slope of the regression line calculated is close to 1 (i.e. 0.98), this 7% overestimation remains constant over the entire range of potential contributions.

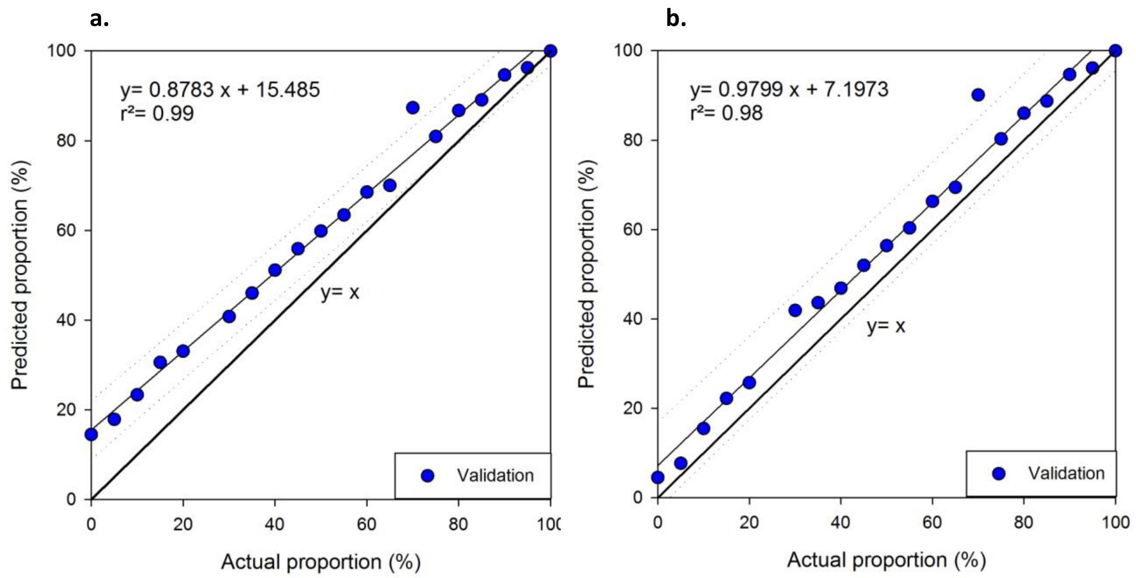

Figure 5 Comparison between actual mining source proportions prepared in artificial mixtures and the mining source proportions predicted by the 'geochemistry' (a) and 'colour + geochemistry' (b) models

3.4 Building partial least-squares models based on FDVS

Mining sources are characterized by a red-orange color while sediments originating from non-mining sources are yellow-grey colour (Figure 1). The colour contrasts may be explained by the distinct geochemical composition of these sources. Mean FDVS indicated the presence of goethite (i.e. at 445 and 525 nm), hematite (i.e. at 555, 565 and 575 nm), and organic matter (i.e. between 600-700 nm) (Debret et al., 2011) in both mining and non-mining sources (Figure ~~4~~6). In similar way, the Thio River sediment samples (2015, 2017) showed similar characteristics since the variations of the mean FDVS remained between those found in the sources (Figure ~~4~~6). Nevertheless, some differences can be observed between the sources. The spectral signature of goethite is slightly stronger at 445 nm in non-mining tributaries compared to mining tributaries. No difference between sources was observed at 525 nm, the second wavelengths characterizing the presence of goethite. In contrast, the spectral signature of hematite (*i.e.* at 555, 565 and 575 nm) was stronger in mining tributaries than in non-mining tributaries.

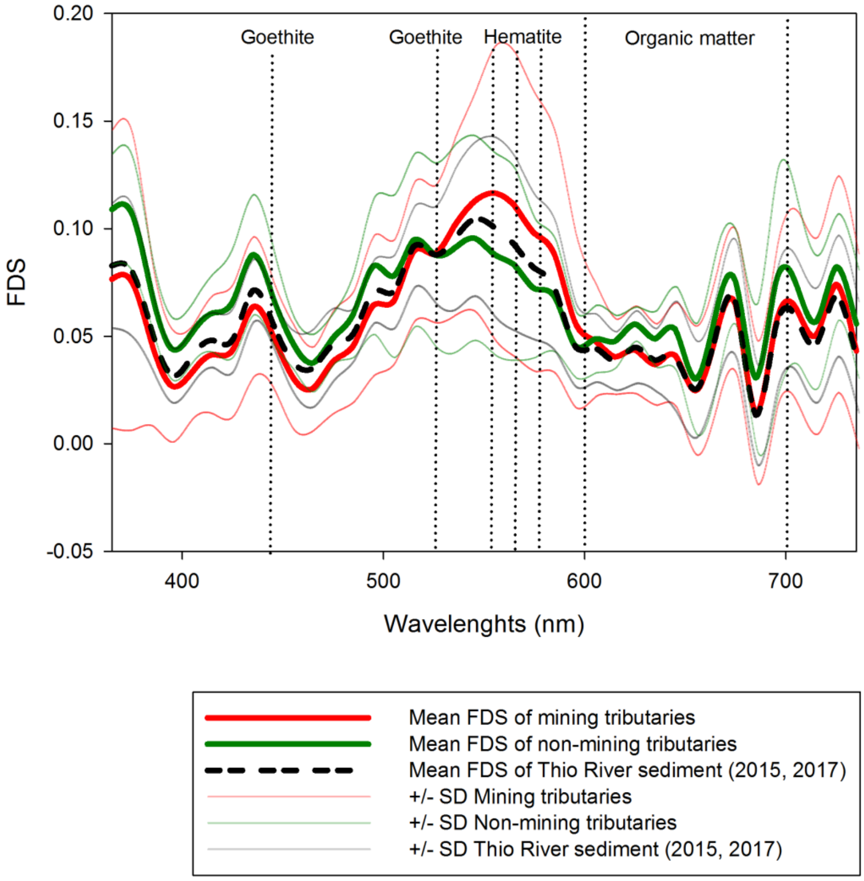

Figure 6 FDVS measured in the <63 µm fraction of sources and Thio River sediment samples

To test the potential discrimination offered by FDVS, a PCA was applied on the source data set. The first ten principal components from PCA explained 99 % of the total variation in the spectra. The DFA performed on these components resulted in a final Wilks' lambda value of 0.1585. It means that 84.1 % of variance is explained by these ten components. Moreover, 100 % of the source samples were correctly classified. The performances of FDVS-PLSR models are presented in Figure ~~5~~7. The mining and non-mining tributary FDVS-PLSR models provided an excellent correlation between actual and predicted proportions with r^2 and slopes close to 1 and intercepts of linear regression close to 0. The root mean square error of calibration (RMSEC) values estimated for both models were low, i.e. 3.4 % and 3.1 % respectively for mining (Figure 7-a) and non-mining tributary models (Figure 7-b). These models also provided a good predictability of source contributions with low root mean square error of prediction (RMSEP) values (i.e. 8.0 % and 4.7 % respectively for mining and non-mining tributary models). Another way to control the reliability of predictions was to sum the predicted proportions of both models (Legout et al., 2013). Considering the whole data set used in the construction of the partial least-squares regression models (i.e. calibration and validation) led to a mean sum of the predicted source proportions of 102 % (SD 3 %, range: 98-114 %), thus highlighting the effective prediction performance of FDVS-PLSR models.

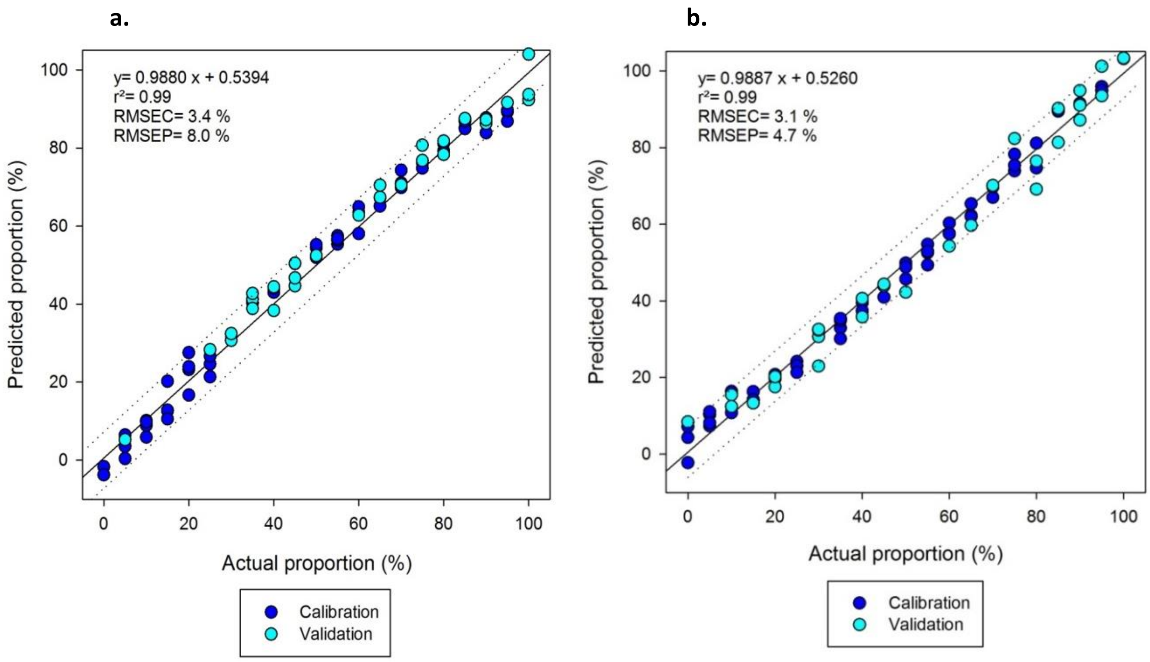

Figure 7 Building of FDSV-PLSR models for mining sources (a) and non-mining sources (b)

3.5 Source apportionment modelling

3.5.1. 'Geochemistry' model

The 'geochemistry' model estimated that the mining tributaries contributed an average of 65 ± 27 % of the Thio River sediment during the 2015 flood event; they therefore dominated sediment inputs overall during this event. Nevertheless, non-mining tributaries mainly contributed to the sediment inputs at three sampling points along the Thio River (Figure ~~6~~8-a, Table 4, sampling points [3, 5, 7]). These contributions did not, however, compensate for those provided by mining tributaries in

the estuary (63-89 %). Indeed, the dominant mining contributions found in upstream river reaches (96 %, Figure ~~6~~8-a, Table 4, sampling point [1]) gradually decreased along the Thio River, fluctuating between 17-77 % before increasing again at the confluence between the Thio River and the mining tributaries draining the Thio Plateau mining area (i.e. 85 %, Figure ~~6~~8-a, Table 4, sampling point [8])
a.
and reaching 60-64 %.

The 'geochemistry' model also demonstrated that mining tributaries dominated sediment inputs with a mean contribution of 83 ± 8% during the 2017 flood event (Table 5). The lowest mining tributary contributions estimated (i.e. 69 %) was found after the confluence with the Kouaré non-mining tributary (Figure ~~6~~8-b, Table 5, sampling point [4]). Nevertheless, further downstream, the proportions of the mining sources increased again to reach 77-83 % in the estuary (Figure 6-b, Table 5, sampling points [7, 8]).

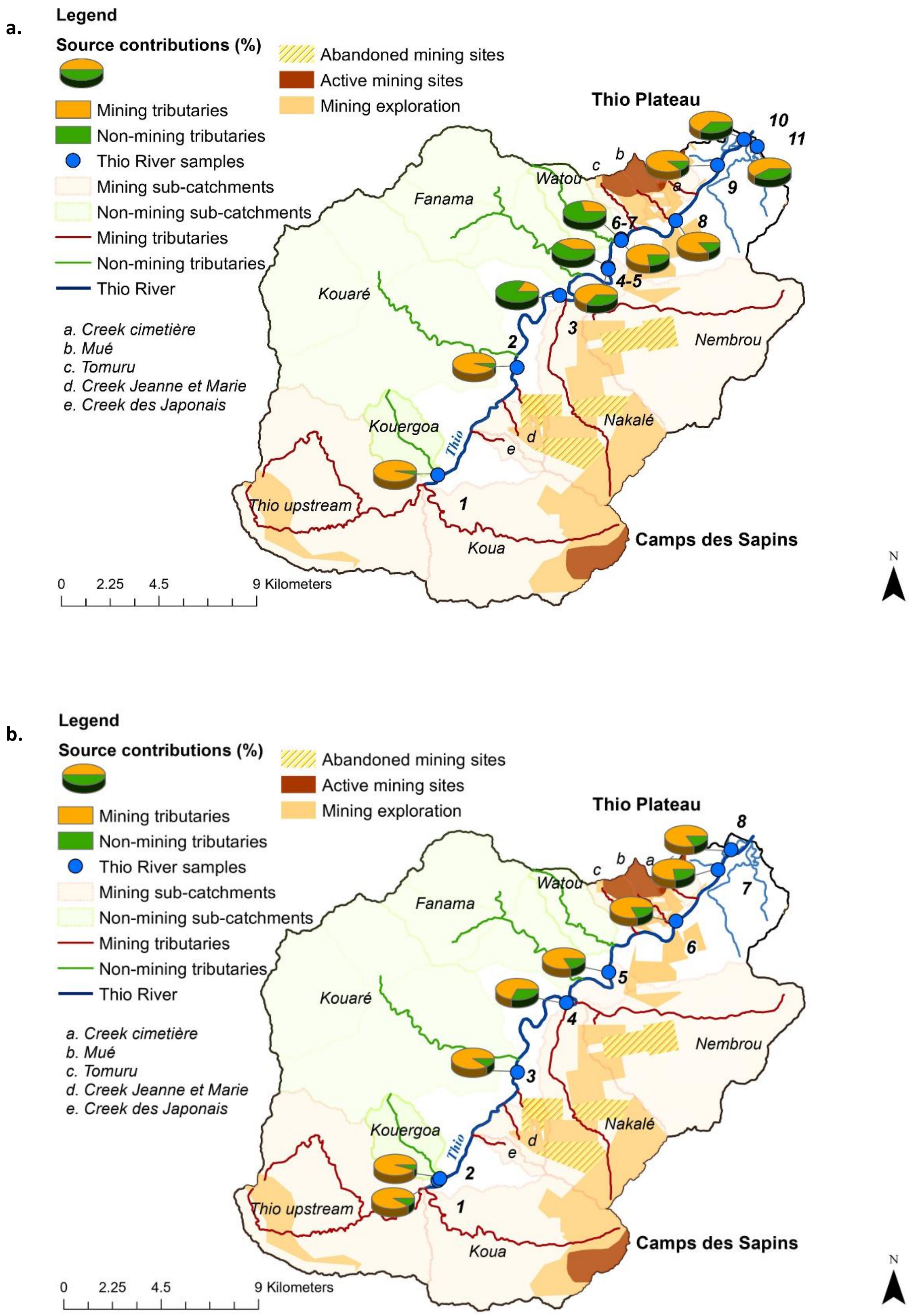

Figure 8 Relative contributions of mining and non-mining tributaries to the sediment collected in the Thio River during the 2015 (a) and 2017 (b) flood events using the 'geochemistry' model

3.5.2. 'Colour + geochemistry' model

Similar results were obtained with the 'colour + geochemisty' model. The contributions of mining tributaries were estimated to an average of 68 ± 25 % for the 2015 flood event. Mining tributary contributions provided almost all the sediment transiting the uppermost reach of the Thio River (i.e. 99 %, Figure ~~7~~9-a, Table 4, sampling point [1]). However, after the confluence with the Kouaré tributary, non-mining tributaries dominated with a contribution of 83 % (Figure ~~7~~9-a, Table 4, sampling point [3]). Further downstream, the contribution of mining tributaries increased again with supplies varying between 34- 89 % to reach 58- 70 % in the estuary (Figure ~~7~~9-a, Table 4). The largest difference between 'geochemistry' and 'colour + geochemistry' model outputs was 18 % for the 2015 flood event.

The 'colour + geochemistry' model also demonstrated that 88 ± 8 % of the sediment supply originated from mining tributaries during the 2017 flood event. Along the Thio River, mining tributary contributions varied between 100 % in the uppermost reach, 74% after the Kouaré river confluence and 83-85% in the estuary (Figure ~~7~~9-b, Table 5). The largest difference between 'geochemistry' and 'colour + geochemistry' model outputs was 10 % for the 2017 flood event (Table 5).

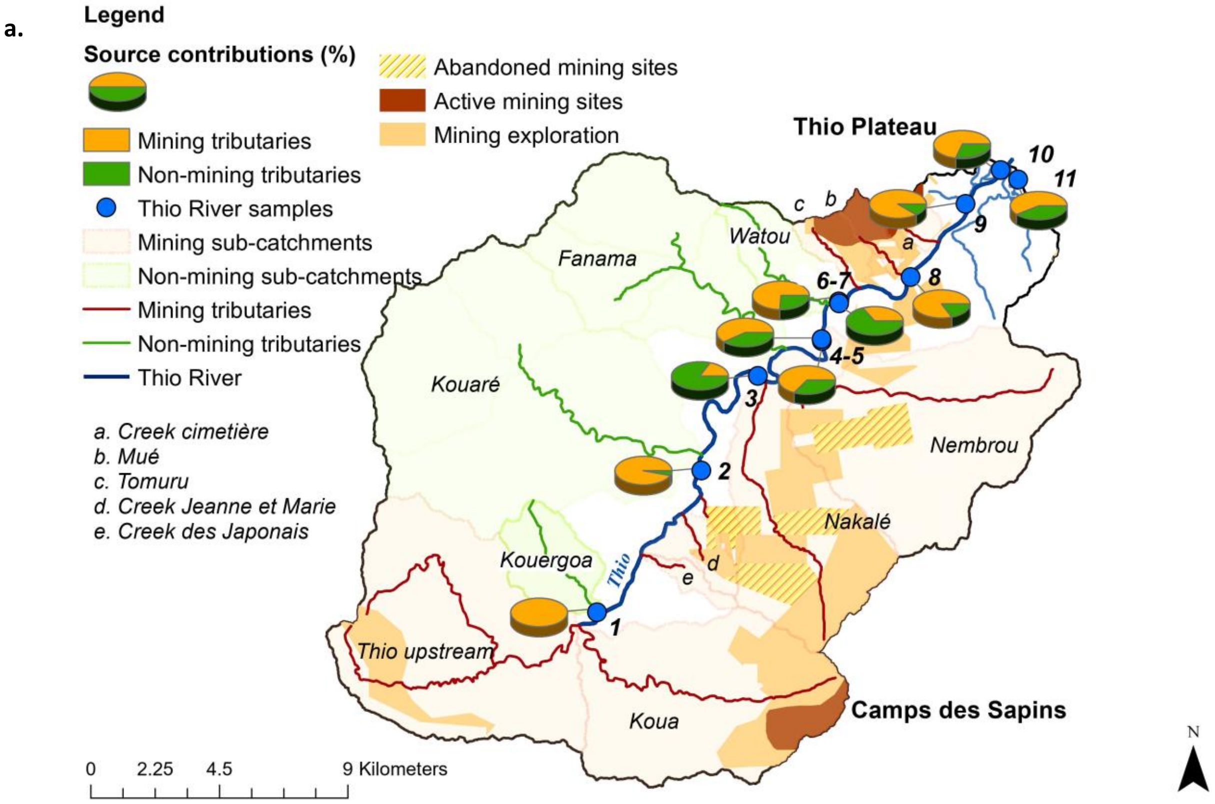

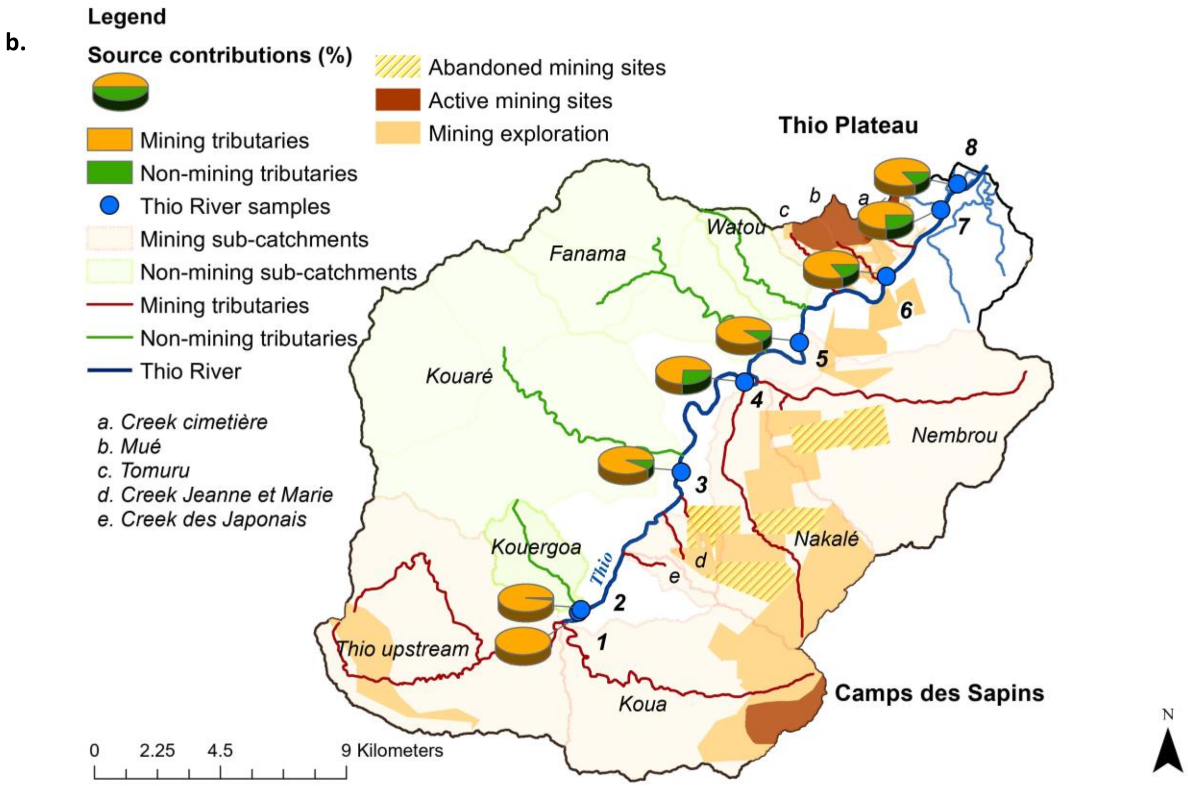

Figure 9 Relative contributions of mining and non-mining tributaries to the sediment collected in the Thio River during the 2015 (a) and 2017 (b) flood events using the 'colour + geochemistry' model

3.5.3. FDVS-PLSR model

Unlike the conventional fingerprinting approach, the estimated contributions of sources were not limited to vary in the range between 0 % and 100 %. In a similar way, the sum of source contributions was not constrained to be equal to 100 %. As a result, another way to control the reliability of predictions was to sum the prediction proportions of both models. For example, if the sum of the source contributions is close to 100 ± 20 % then it likely indicates that no source is lacking. On the contrary, it is likely that a source has not been sampled and included in the study or that the behaviour of the fingerprinting properties is not conservative (Legout et al., 2013). When applying the FDVS-PLSR models (i.e. mining and non-mining tributary contributions) to the river sediment samples (2015, 2017), the mean sums of the source contributions were 92 ± ~~% (SD~~ 8 %~~)~~ and 80 ± ~~% (SD~~ 13 %~~)~~, respectively, for the 2015 and 2017 flood events (Tables 4 and 5) which are satisfactory results. However, for the 2017 flood events, three river sediment samples collected on sampling points n°1, 2 and 3 showed sums of source contributions below 70 %, indicating a lack of reliability of the model. The results obtained on these three points must therefore be interpreted with great caution. Moreover, and owing that predicted sums were slightly different from the expected 100 %, a bar plot display of the source contributions has been chosen to facilitate the interpretation of the results (Figure ~~8~~10).

According to the FDVS-PLSR model results, 34 ± ~~% (SD~~ 22 %~~)~~ of sediment supply originated from mining tributaries while non-mining tributary contribution provided 58 ± ~~% (SD~~ 18 %~~)~~ of the sediment input for the 2015 flood event (Figure ~~8~~10-a, Table 4). In the upper part of the Thio River catchment, non-mining tributaries largely dominated with a contribution of 80 % versus 6 % for mining tributaries. Along the Thio River, mining tributary contributions gradually increased to reach 70 % after the Mué tributary confluence (i.e. one of tributaries draining the Thio Plateau Mine, Figure 8-a, Table 4, sampling point [9]). The non-mining tributary contributions fluctuated along the Thio River between 41-85 % (Figure 8-a, Table 4, sampling points [2-8]) and reached a minimum to 28 % (Figure ~~8~~10-a, Table 4, sampling point [9]) after the Mué tributary confluence. In the estuary, sediment supply was originated from 51-70 % of mining tributaries and 28-~~-~~52 % of non-mining tributaries (Figure ~~8~~10-a, Table 4, sampling points [9, 10, 11]).

The FDVS-PLSR models also indicated that mining and non-mining tributaries respectively contributed a mean of 29 ± ~~% (SD~~ 20 %~~)~~ and 51 ±~~% (SD~~ 11 %~~)~~ of sediment (Figure ~~8~~10-b, Table 5) during the 2017 flood event. In a similar way, mining contributions gradually increased along the Thio River from 11 % in upper parts to reach 52-58 % in the estuary. On the contrary, non-mining contributions gradually decreased from 56 % in uppermost parts to reach 35-36 % in the estuary (Figure ~~8~~10-b, Table 5).

In summary, the FDVS-PLSR models provided opposite results to those of the conventional sediment fingerprinting approach (i.e. 'geochemistry' and 'colour + geochemistry' models). According to the FDVS-PLSR models, non-mining tributaries contributed the majority of the sediment supply for the 2015 (58 ± ~~%, SD~~ 18 %) and 2017 (51 ± ~~%, SD~~ 11 %) flood events. On the contrary, the 'geochemistry' and 'colour + geochemistry' models demonstrated that mining tributary contributions dominated sediment supply for the 2015 (i.e. respectively 65 ± ~~% (SD~~ 27% ~~)~~ and 68 ± ~~% (SD~~ 28 %~~)~~) and 2017 flood events (i.e. respectively 83 ±~~% (SD~~ 8%) and 88 ±~~% (SD~~ 8%~~)~~).

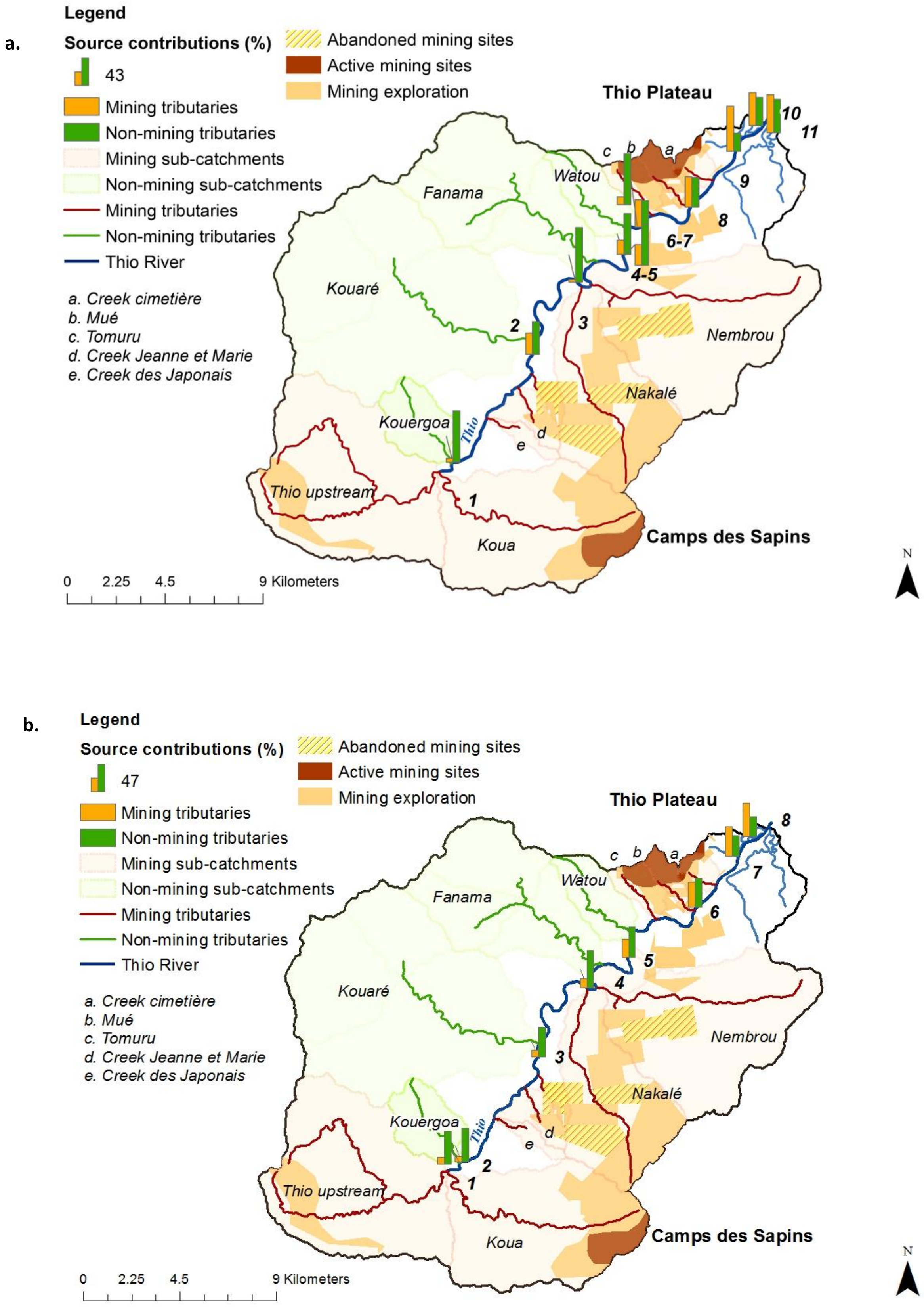

Figure 10 Relative contributions of mining and non-mining tributaries to the sediment collected in the Thio River during the 2015 (a) and 2017 (b) flood events using the FDVS-PLSR models

Table 4 Source contributions calculated by FDVS-PLSR, 'geochemistry', 'colour + geochemistry' approaches for sediment deposited during the flood of February 25,2015 (Mean, SD: standard deviation, minimum, maximum)

	Mining tributary contributions (%)			Non-mining tributary contributions (%)			Sum of source contributions (%)		
Sampling point	FDS- PLSR	Geochemistry	Colour + Geochemistry	FDS- PLSR	Geochemistry	Colour + geochemistry	FDS- PLSR	Geochemistry	Colour + geochemistry
1	6	96	99	80	4	1	86	100	100
2	33	95	96	51	5	4	84	100	100
3	4	17	17	85	83	83	90	100	100
4	32	65	65	64	35	35	96	100	100
5	22	41	59	63	59	41	85	100	100
6	42	77	74	41	23	26	83	100	100
7	12	29	34	79	71	66	91	100	100
8	47	85	83	46	15	17	93	100	100
9	70	88	89	28	12	11	98	100	100
10	51	64	70	44	36	30	94	100	100
11	59	60	58	52	40	42	111	100	100
Mean (%)	34	65	68	58	35	32	92	100	100
SD (%)	22	27	25	18	27	25	8	-	-
Minimum (%)	4	17	17	28	4	1	84	-	-
Maximum (%)	70	96	99	85	83	83	111	-	-

Table 5 Source contributions calculated by FDVS-PLSR, 'geochemistry', 'colour + geochemistry' approaches for sediment deposited during the flood of April 10,2017 (Mean, SD: standard deviation, minimum, maximum)

	Mining tributary contributions (%)			Non-mining tributary contributions (%)			Sum of source contributions (%)		
Sampling point	FDS- PLSR	Geochemistry	Colour + Geochemistry	FDS- PLSR	Geochemistry	Colour + geochemistry	FDS- PLSR	Geochemistry	Colour + geochemistry
1	11	90	100	56	10	0	66	100	100
2	9	94	98	58	6	2	68	100	100
3	11	89	92	52	11	8	63	100	100
4	16	69	74	66	31	26	82	100	100
5	32	82	89	54	18	11	86	100	100
6	44	81	84	51	19	16	95	100	100
7	52	77	83	36	23	17	88	100	100
8	58	83	85	35	17	15	92	100	100
Mean (%)	29	83	88	51	17	12	80	100	100
SD (%)	20	8	8	11	8	8	13	-	-
Minimum (%)	9	69	74	35	6	0	63	-	-
Maximum (%)	58	94	100	66	31	26	95	-	-

3.6 Complementary tests: representativeness of artificial mixture samples used for the FDVS-PLSR models compared to source samples

~~Given the opposite results obtained in terms of source contributions between FDVS-PLSR models on the one hand and 'geochemistry' and 'colour + geochemistry' models on the other hand, complementary analyses were carried out on individual source samples (i.e. not the composite samples used to create the artificial mixtures) to estimate their composition in terms of source contributions with FDVS-PLSR models. As done in Legout et al. (2013) to assess uncertainties in the fingerprinting approach due to source heterogeneity, they were considered as river sediment samples.~~ The FDVS-PLSR models provided contradictory results compared to those obtained with the 'geochemistry' and 'colour + geochemistry' models. In order to explain these results, complementary analyses were carried out with this model. This model was built from the mining and non-mining tributary samples (i.e. mixture of source samples > source poles > artificial mixture samples > FDVS-PLSR models). The objective of these analyses was to check whether the model is 'well built', in other words whether it is representative of the sources identified and whether it is capable of correctly 'classifying' the sources. To this end, we applied the FDVS-PLSR models on source samples to estimate their composition in terms of source contributions with FDVS-PLSR models. In the same way as we did above for the river sediment samples, we assessed the reliability of predictions by summing the source contributions predicted by both models (Legout et al., 2013). A mean sum of the predicted source proportions of 94 ± ~~% (SD~~ 17 %~~)~~ was calculated from the source sample data set which again is an excellent result. However, for the three mining tributary samples collected on the Koua tributary, the corresponding sums remained below 65 % with a minimum of 49% whereas for one of the non-mining tributary sample collected on the Kouaré tributary, the sum reached 131% (Figure 11). These results indicate that the FDVS-PLSR models provide unreliable predictions when dealing with river sediment samples with a colour signature partly due to these four samples. The colorimetric signature of the mining tributary samples collected on the Koua tributary in particular is not fully recognized by the models. The compositions of mining and non-mining tributary samples in Figures ~~9~~ 11 and ~~10~~ 12 also show that artificial mixture samples built from a mix between the composite mining source sample and the composite non-mining source sample did not cover entirely the range of values found in all the sources samples which may explain why some source samples showed mining and non-mining tributary composition lower than 0 and/or higher than 100 %.

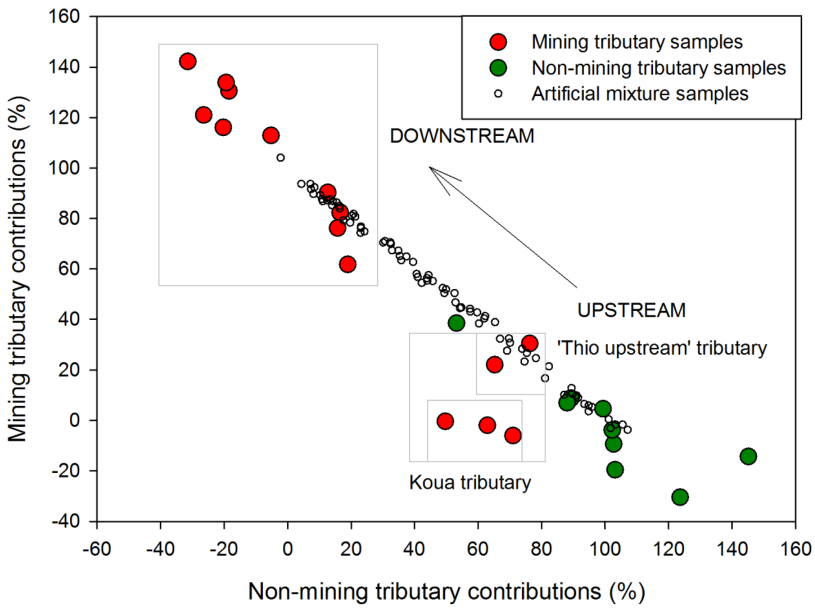

Figure 11 Relative compositions of mining and non-mining sources estimated by the FDVS-PLSR models applied to the individual source sediment samples

Moreover, we observed that two sub-groups of mining tributary samples can be distinguished, the first one corresponding to samples collected on the mining tributaries located in the uppermost part of the catchment and the second to samples collected on the mining tributaries located further downstream. The FDVS-PLSR differentiated rather well the second group since the mining tributary composition is dominant in these samples. On the contrary, the first group referred to as ‘Upstream’ merged with the non-mining tributary samples (Figure ~~9~~11). Indeed, Figure ~~10~~ 12 shows the mining tributaries located in the upper part of the catchment were defined as ‘non-mining tributaries’ by the FDVS-PLSR models.

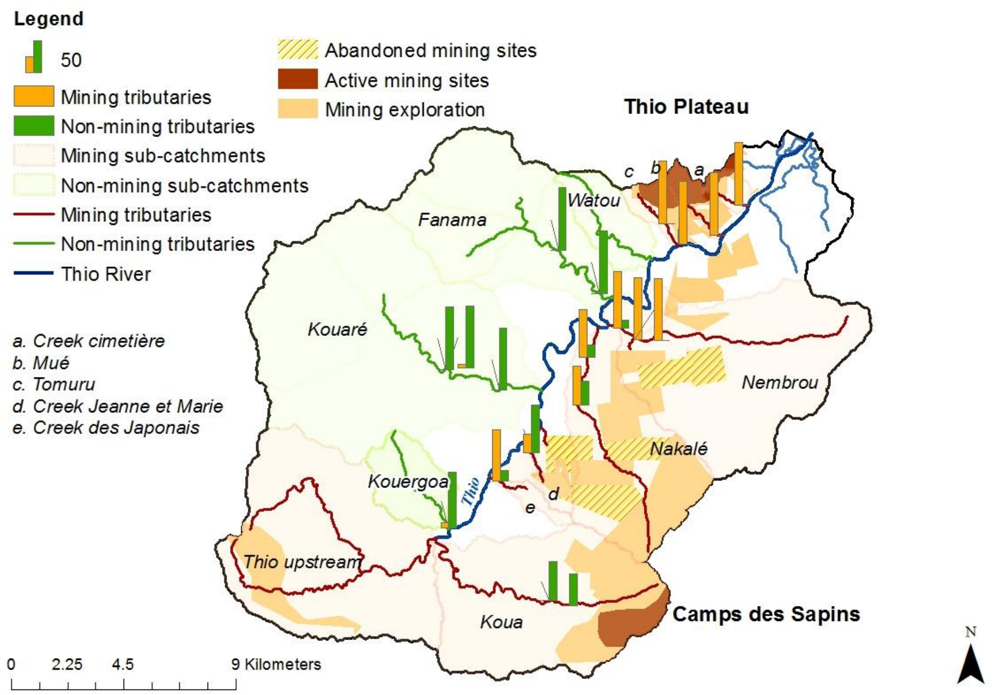

Figure 12 Relative compositions of mining and non-mining sources estimated by the FDVS-PLSR models applied to the individual sediment sources in the Thio River catchment

The low K contents found in these samples confirmed, however, that they were mainly supplied by mining sources (Figure ~~11~~13). Indeed, only tributaries draining peridotite massifs (i.e. mining areas) can show such low K contents in source samples (Sellier et al., 2019). Nevertheless, a colour difference could be observed visually and through variations of the a* parameter: the a* values increased from upper parts to lower, which results in an increasingly red coloration of mining tributary samples in downstream direction. Figure ~~11~~ 13 shows also that the a* values found in samples collected in the upper catchment part overlapped with those of non-mining tributary samples. ~~Among the 'upstream' mining tributary samples, only three samples collected on the Koua tributary (i.e. draining Camps des Sapins mine) showed values that were not comprised in the ranges covered by the artificial mixture samples (Figure 9).~~

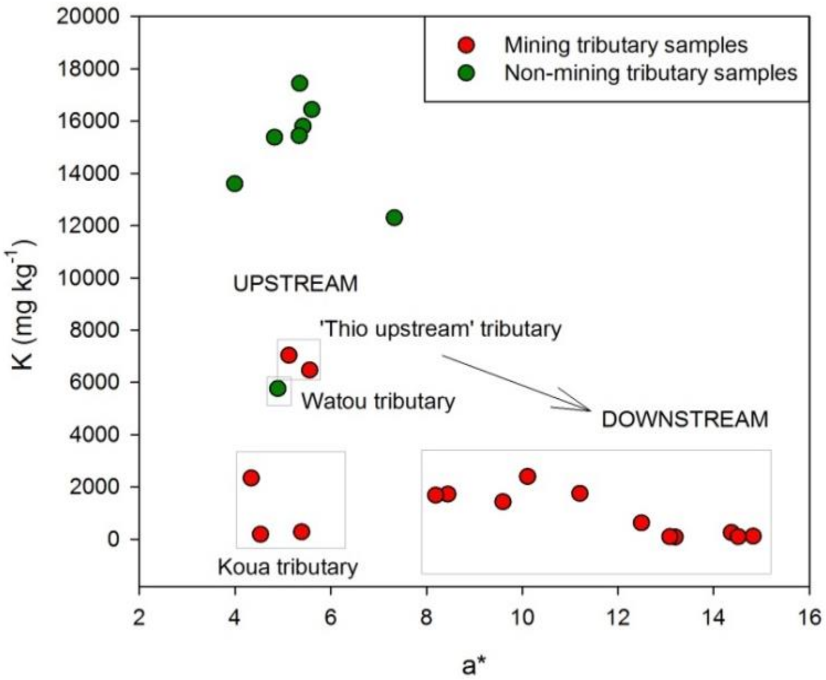

Figure 13 Diagram of K contents as a function of a* parameter values within sediment sources and artificial mixture samples

4.Discussion

4.1.Advantages and limits of models

4.1.1. 'Colour' model

One of the objectives of this study was to test the contribution of spectrocolorimetry for improving the source discrimination. Indeed, visual observations indicated that mining tributary samples were red-orange whereas non-mining tributary samples were rather yellow-grey (Figure 1). However, the results showed that the colour parameters, when used individually, did not provide sufficient discrimination between sources (Table 2) to meet this objective. Indeed, some mining tributary samples showed colour parameter values similar to those found in non-mining tributary samples (e.g. v' at Table 3, or a* shown at Figure ~~11~~13). This overlap of value ranges could explain in particular the inability of the 'colour' model to provide satisfactory source discrimination. In the case of mining sources, minerals such as hematite or goethite provide them their reddish-orange colour (Quantin et al., 1997). Indeed, hematite is a red coloured oxidized mineral while goethite is a yellow coloured oxidized mineral (Trescases, 1973). According to Figure 6, non-mining tributary samples also have high contents of goethite which could interfere with the discrimination of the colour signatures of the two sources. The non-mining tributaries drain areas devoid of mining activities mainly located on the volcano-sedimentary formation rocks. The soil-geological profiles within the volcano-sedimentary formation rocks are characterized at the surface by clay horizons and at depth by oxidized horizons enriched in goethite in particular (Denis, 1988). According to Sellier et al. (2019), subsurface erosion processes dominate in the Thio River catchment. In other words, landslides mainly contribute to non-mining sediment inputs. As a result, the oxidized horizons of these rock formations are also likely subject to erosion processes which could explain the occurrence of goethite and material with a yellow-grey color in non-mining tributary samples.

~~Nevertheless~~ Moreover, results obtained with colour parameter analyses coupled to visual observations highlighted the occurrence of two groups of mining tributary samples (i.e. ‘Upstream’ and ‘Downstream’). The coloration differences (i.e. orange/ ‘Upstream’ and ‘red/Downstream’) observed between these two groups could be due to the the fact that on the one hand, the reddish colour does not provide a highly conservative signature as it may be altered by the oxydo-reduction of iron minerals during the periods of submersion of sediments under water. On the other hand, the presence of different types of nickel ores could explain these coloration differences. Indeed, the laterite profile is classically described in the literature as composed of peridotites at the bottom > saprolites > yellow laterites rich in goethite > red laterites rich in hematite at the top (Trescases, 1973). However, certain minor features may be found in the laterite profile depending on the type of parent rock found at the base of the peridotite massifs (Sevin, 2014). The mineral composition found in the different layers of the laterite profile may vary depending on whether serpentines or peridotites are the source rocks. Moreover, nickel ore formation depends partly on the morphological context, for instance on whether nickel ores are located in a basin, on a plateau or a slope. This morphological context influences the weathering level of peridotites and the formation of laterite profile: the more the laterite profile is altered, the higher the thickness of red laterites. In the Thio River catchment, nickel ores from the Thio Plateau mine located in the downstream part of the catchment are 'plateau nickel ores' whereas those from the Camps des Sapins mine located in the upstream part of the catchment are 'slope nickel ores' (Mardhel et al., 2018). No information is provided in the literature on the types of nickel ores that were mined in abandoned mining sites. The red coloration of the 'Downstream' mining tributary samples could then be associated with more altered laterite profiles with a thicker layer of red laterites characteristic of 'plateau nickel ores' compared to the 'Upstream' mining tributary samples, which could be associated with a laterite profile with a thinner layer of red laterites characteristic of 'slope nickel ores'. The red laterites are the final stage of alteration of the peridotite massifs. It therefore appears likely that the less altered 'slope nickel ore' probably contains more yellow laterites enriched in goethite compared to the 'plateau nickel ore'. This hypothesis could explain the similar colour signature of the mining tributary samples collected on the Koua tributary draining the Camps des Sapins mine and the non-mining samples.

4.1.2. 'Geochemistry' model

The 'geochemistry' model based on K provided significant discrimination between sources (Table 2), regardless of the types of nickel ores that may be found in the Thio River catchment. K is a lithological tracer discriminating sediments originating from the erosion of the two dominant lithologies (i.e. peridotite massifs vs. volcano-sedimentary formations) in the Thio River catchment. As anthropogenic erosion (i.e. due to mining activities) dominates on the peridotite massifs (Garcin et al., 2017), K therefore provides an optimal discrimination between mining and non-mining tributary contributions.

This parameter classified the source samples rather well (i.e. 95.3 % of correct classification, Table 3). Indeed, the 16 mining source samples were all correctly classified (100%) and only one non-mining source sample was not correctly classified (87.5 %); it corresponds to the Watou tributary sample (Figure ~~11~~13). This sample showed a K content similar to that found in mining tributary samples. The Watou tributary is particular because it drains both volcano-sedimentary formations and peridotite massifs that were not exploited for mining, which justifies that it was considered as a non-mining tributary. The K content measured in this sample could be representative of that found in sediment sources characterized by a mix between the two dominant lithologies. Again, when observing Figure ~~11~~13, two mining tributary samples (i.e. 'Thio upstream') showed similar K contents to that found in the Watou tributary sample. The 'Thio upstream' tributary also drains both areas associated with volcano-sedimentary formations and exploited peridotite massifs (i.e. mining prospection), which justifies that it was considered as a mining tributary.

The analysis of colour parameters coupled with that of geochemical elements indicated that these samples collected on the 'Thio upstream' tributary showed a less red coloration not because they are associated with a different type of ore, as could be the case for the samples collected on Koua tributary draining Camps des Sapins mine (Figure ~~11~~13), but because they are characterized by a mix of both lithologies. As a result, the 'geochemistry' model showed a certain limitation to classify source samples characterized by a mix of both lithologies. The performance of the 'geochemistry' model described in Table 2 remains, however, excellent. The application of this model on artificial mixture samples provided very satisfactory results (Figure ~~3~~5-a) with a good correlation between the predicted and the actual source proportions (r^2= 0.99). Estimations of mining tributary contributions may, however, be overestimated. This overestimation evaluated to a maximum at 15.5 % is greater when the mining contributions estimated by the model tend towards 0 % (maximum: 15.5 %, Figure 3-a). The 'geochemistry' model has difficulties to discriminate sediment contributions from sub-catchments with mixed lithologies. It classifies these types of samples as originating from mining tributaries, such as the Watou River sample. As a result, as the K concentrations decrease in the samples analyzed, the model will tend to overestimate the contributions of mining sources by default compared to their actual contributions.

~~4.1.3.~~

~~4.1.4.~~4.1.3. 'Colour + geochemistry' model

The 'colour + geochemistry' (i.e. K, Ca, Ti, b*, C*) model provided the best discrimination between sources (Table 3). The inclusion of colour parameters in the 'colour + geochemistry' approach allowed for the discrimination of source samples (i.e. 100 % of correctly classified source samples) that a 'geochemistry' approach alone could not achieve. Results of the tests carried out on the artificial mixture samples also showed an excellent correlation between the predicted and the actual source proportions (i.e. r^2= 0.98). A slight overestimation of the mining tributary contributions (7 %) was observed with this approach, which remains rather reasonable (Figure 3-b). In this model, K is the lithological tracer which has the higher discriminant powerful (Table 2), which may explain the similarity of results obtained with the 'colour + geochemistry' and the 'geochemistry' models. Indeed, mining tributaries contributed an average of 65 ± ~~% (SD~~ 27 %~~)~~ for 'colour + geochemistry' model and 68 ± ~~% (SD~~ 25 %~~)~~ for 'geochemistry' model (Table 4). For the 2017 flood event, mining source contributions largely dominated the sediment production with a mean contribution of 83 ± ~~% (SD~~ 8 %~~)~~ for the 'geochemistry' model and 88 ± ~~% (SD~~ 8 %~~)~~ for the 'colour + geochemistry' model.

~~4.1.5.~~4.1.4. FDVS-PLSR models

The FDVS-PLSR models built from artificial mixture samples showed excellent theoretical predictive performances (e.g. r^2, RMSEC, RMSEC, Figure ~~5~~7). However, the application of these models on river sediment samples provided questionable results. Indeed, the artificial mixture samples did not cover entirely the ranges of values found in all sources samples, thus resulting in an overestimation (i.e. superior to 100 %) and an underestimation (i.e. inferior to 0 %) of source composition (Figure ~~9~~11) in several source samples. Similarly to what was previously observed, three sub-groups of mining tributary samples can be distinguished, one of which (i.e. 'Thio Upstream') is partially merged with the non-mining tributary samples (Figure ~~9~~11). When modelling the source contributions with the FDVS-PLSR models, a bias was created because the contributions of the 'Thio upstream' tributary may be mainly considered as the contributions of non-mining tributaries. As a result, an overestimation of non-mining tributary contributions may be found in the entire Thio River catchment and particularly in the upper part of the study area. Third, the properties measured in the Koua tributary (i.e. draining Camps des Sapins Mine) samples were not comprised in the ranges of values covered by the artificial mixture samples (Figure ~~9~~11).

Given the particular colour signature of this tributary (Figure ~~11~~13), its contributions are therefore not taken into account at all by the FDVS-PLSR models. Indeed, the sums of the source contributions by FDVS-PLSR models are lower than the expected 100% particularly in the uppermost part of the catchment (Tables 4 and 5), which may indicate that a source is not accounted for. Artificial mixtures were constructed from a homogenized spectral signature of all mining source samples. However, two distinct spectral signatures were observed between the upstream and downstream mining source samples. Homogenizing the spectral signature of the mining samples led to a loss of information in terms of spectral signature, in particular that of the mining samples located upstream. As a result, a 3-source FDVS-PLSR models (i.e. non-mining, upstream and downstream mining sources) would have been more appropriate than 2-source FDVS-PLSR models in this context.

4.2. Spatial and temporal variations of sediment source contributions

Among the four models tested in this study, the 'colour + geochemistry' model is the most appropriate to estimate mining and non-mining tributary contributions in the Thio River catchment. According to the results of this model, mining tributaries provided the main sediment supply to the river system with a mean contribution of 68 ± ~~% (SD~~ 25 %~~)~~ for the 2015 flood event and 88 ± ~~% (SD~~ 8 %~~)~~ for the 2017 flood event (Tables 4 and 5). The variability of mining tributary contributions between these two flood events with a return period of 10 years (3500 $m^3 s^{-1}$) could be explained in particular by the variability of rainfall distribution (Sellier et al., 2019). Indeed, during the 2015 flood event, the Kouaré River sub-catchment received twice the rainfall than observed in the rest of the Thio River catchment, which may explain a higher contribution of non-mining tributaries for this event than for the 2017 flood event where rainfall was more intense on the eastern part of the catchment in the vicinity of the mines currently in operation (Thio Plateau, Camps des Sapins). In addition, the inhabitants of Thio reported that bushfires had occurred in the Kouaré and Fanama sub-catchments in 2015, which could have led to an increase in soil erosion processes, particularly landslides, in these sub-catchments. This could also explain why the sediment contributions of the Kouaré tributary are higher in 2015 compared to 2017. However, it is likely that, as for low intensity floods (i.e. <200 $m^3.s^{-1}$), sediment generated during previous floods has been remobilized (Allenbach et al., 2020). The current research does not allow to quantify this proportion of remobilized sediments. Future studies based on the measurement of the $^7Be/^{210}Pb_{xs}$ ratio could provide information on this question as both isotopes are supplied by rainfall and ^7Be is short-lived while $^{210}Pb_{xs}$ is much longer-lived. Indeed, this ratio has been used in previous research to determine whether sediment has been eroded recently (i.e. with a high ratio of $^7Be/^{210}Pb_{xs}$) or whether they have been remobilized from the channel (i.e.with a low ratio of $^7Be/^{210}Pb_{xs}$) (Le Gall et al., 2017;Evrard et al., 2015).

Although the FDVS-PLSR models were unable to properly estimate the source contributions, they provided qualitative indications about the proportion of sediment contribution between 'Upstream' and 'Downstream' mining tributaries at the level of the estuary. Indeed, only 'downstream' mining tributaries were finally identified by the FDVS-PLSR models as mining sources. Mining contributions gradually increased in downstream direction. The predicted proportion sums of river sediment samples also tend to reach the expected 100 %, which could result in a better predictability of the models. As a result, these models indicated that sediment contribution from downstream reaches dominated that of upstream reaches at the level of the estuary for both events.

Moreover, the analysis of colour parameters coupled to that of geochemical elements highlighted the occurrence of three sub-groups of mining tributary samples, (1) 'Downstream' samples characterized by high a* values and low K contents, (2) 'Koua tributary' samples located in the upstream characterized by low a* values and low K contents and (3) 'Thio upstream' samples corresponding to a mix of both dominant lithologies (i.e. peridotite massifs and volcano-sedimentary formations) characterized by low a* values and higher K contents (i.e. 4 times higher than for the two previous sub-groups) (Figure ~~11~~13). Owing to the low K contents found in Thio River sediment samples collected in the uppermost part (i.e. ~ 2200 mg kg^{-1} in 2015 and ~ 2600 mg kg^{-1} in 2017), which were similar to those measured in samples of sub-group (2) (~2400 mg kg^{-1}), it would appear that the Koua tributary draining Camps des Sapins mine dominated the sediment supply in the upstream for both events.

Conclusions

The current study showed that the contributions of mining sources dominated the sediment inputs with mean contributions of 68 ± ~~% (SD~~ 25 %~~)~~ for the 2015 flood event and 88 ± ~~% (SD~~ 8 %~~)~~ for the 2017 flood event (results of 'colour + geochemistry' model). Although the spatial variability of rainfall may impact local sediment source contributions, a trend in terms of sediment source contributions is observed along the Thio River for both flood events. In the uppermost part of the catchment, mining source contributions dominated (99% in 2015, 100% in 2017) with a dominant contribution from the Koua tributary draining the Camps des Sapins mine. The first non-mining tributary encountered in downstream direction (i.e. the Kouergoa tributary) contributed little to sediment supply; it is rather the next non-mining tributaries (i.e. the Kouaré tributary) which provided most of the sediment inputs (83 % in 2015, 26 % in 2017). Nevertheless, these contributions were compensated in downstream direction by those from mining sources generated by tributaries draining Thio Plateau mine. Finally, at the estuary, mining sources dominated (58-70 % in 2015, 83-85 % in 2017). These results therefore suggest that catchment management should focus on mining tributaries draining active mining sites (i.e. Camps des Sapins and the Thio Plateau) and the Kouaré tributary for the non-mining tributaries.

One of the objectives of this study was to evaluate the performance of sediment tracing methods based on spectroscopy measurements (i.e. colour parameters and FDVS). The results showed that these individual fingerprinting approaches did not provide sufficient discrimination between sources to be used for the modelling of sediment source contributions. Nevertheless, the inclusion of colour properties in addition to geochemical parameters turned out to be the optimal combination of tracers providing the highest discrimination between sediment sources. This 'colour + geochemistry' model is, however largely based on the discriminatory power provided by K, which means that the 'geochemistry' approach is also relevant to quantify sediment sources. Both approaches have, moreover, been experimentally validated. As a result, the use of these approaches could be extended to other mining catchments of New Caledonia but also possibly to other similar nickel mining catchments (i.e. Ni oxidized ores based on peridotite massifs) around the world.

Data availability

The database has been registered on the PANGEAE website and is currently undergoing the editorial process: https://issues.pangaea.de/browse/PDI-25229.

Author contribution

Oldrich Navratil, Michel Allenbach and Olivier Evrard designed research. Virginie Sellier, Oldrich Navratil, Olivier Evrard and Irène Lefèvre carried out fieldwork sampling. Virginie Sellier conducted the analyses. All co-authors contributed to data analysis and interpretation. John Patrick Laceby contributed to modelling. All co-authors contributed to the writing and approved the final version of the manuscript.

Competing interests

The authors declare that they have no conflict interest.

Acknowledgements

This work was funded by the National Technical Research Center (CNRT) “Nickel and Its Environment”, Noumea, New Caledonia » (n°10PS2013-CNRT.UNC/IMMILA). The PhD project of Virginie Sellier is also financed by the French Atomic Energy Commission (CEA, Commissariat à l’Energie Atomique et aux Energies Alternatives). The authors are grateful to Jean-Guy M’Boueri, Pierre Chanel, Jean-Jean, Lorenza M’Boueri, Nicolle Mathys for their invaluable support to identify and have access to the field sampling sites. The authors would also like to thank Magdalena Uber for her contribution to the spectrocolorimetric analyses.

References

Abel, A., Michael, A., Zartl, A., and Werner, F.: Impact of erosion-transported overburden dump materials on water quality in Lake Cospuden evolved from a former open cast lignite mine south of Leipzig, Germany, Environmental Geology, 39, 683-688, 2000.

Allenbach, M., Bertrand, M., Despinoy, Y., Evrard, O., Garcin, M., Liébault, F., Navratil, O., Recking, A., Richard, D., Rouet, I., Sabinot, C., Sellier, V., Tessier, B., Thinon, I., Touraivane, and Worliczek, E.: Rapport scientifique. Programme « IMMILA, Impact de la mine au lagon ». CNRT « Nickel & son environnement. 250 pages. , 2020.

Batista, P. V. G., Laceby, J. P., Silva, M. L. N., Tassinari, D., Bispo, D. F. A., Curi, N., Davies, J., and Quinton, J. N.: Using pedological knowledge to improve sediment source apportionment in tropical environments, J Soils Sediments, 10.1007/s11368-018-2199-5, 2018.

Baudrimont, M., Dominique, Y., Feurtet-Mazel, A., Gonzalez, P., Gourvès, P.-Y., Gunkel-Grillon, P., Laporte-Magoni, C., Lefrançois, E., Letourneur, Y., Marquié, J., Maury-Brachet, R., Monna, F., Pasquet, C., Rivière, E., and Roth, E.: - Rapport scientifique final. Programme « Dispersion des métaux de la mine au lagon. ». CNRT « Nickel & son environnement ». 192 pages, 2019.

Bird, E. C. F., Dubois, J. P., and Iltis, J. A.: The impacts of opencast mining on the rivers and coasts of New Caledonia. Tokyo, Japan, United Nations University, 1984.

Blake, W. H., Wallbrink, P. J., Wilkinson, S. N., Humphreys, G. S., Doerr, S. H., Shakesby, R. A., and Tomkins, K. M.: Deriving hillslope sediment budgets in wildfire-affected forests using fallout radionuclide tracers, Geomorphology, 104, 105-116, 10.1016/j.geomorph.2008.08.004, 2009.

Brosinsky, A., Foerster, S., Segl, K., and Kaufmann, H.: Spectral fingerprinting: sediment source discrimination and contribution modelling of artificial mixtures based on VNIR-SWIR spectral properties, Journal of soils and sediments, 14, 1949-1964, 2014.

Brown, A.: The potential use of pollen in the identification of suspended sediment sources, Earth Surface Processes and Landforms, 10, 27-32, 1985.

Clarke, P., and David, C.: New Provincial Environmental Legislation in New Caledonia: Continuity and Reform in Environmental Governance in a French Pacific Territory, Asia Pac. J. Envtl. L., 13, 135, 2010.

Collins, A., and Walling, D.: Selecting fingerprint properties for discriminating potential suspended sediment sources in river basins, Journal of hydrology, 261, 218-244, 2002.

Collins, A. L., Walling, D. E., and Leeks, G. J. L.: Composite fingerprinting of the spatial source of fluvial suspended sediment : a case study of the Exe and Severn river basins, United Kingdom, Géomorphologie, 2, 41-53, 10.3406/morfo.1996.877, 1996.

Coulthard, T. J., and Macklin, M. G.: Modeling long-term contamination in river systems from historical metal mining, Geology, 31, 451-454, 2003.

Danloux, J., and Laganier, R.: Classification et quantification des phénomènes d'érosion, de transport et de sédimentation sur les bassins touchés par l'exploitation minière en Nouvelle Calédonie, 1991.

Daszykowski, M., Walczak, B., and Massart, D.: Representative subset selection, Analytica chimica acta, 468, 91-103, 2002.

Davis, C. M., and Fox, J. F.: Sediment fingerprinting: review of the method and future improvements for allocating nonpoint source pollution, J Environ Eng, 135, 490-504, 2009.

Debret, M., Sebag, D., Desmet, M., Balsam, W., Copard, Y., Mourier, B., Susperrigui, A.-S., Arnaud, F., Bentaleb, I., and Chapron, E.: Spectrocolorimetric interpretation of sedimentary dynamics: the new “Q7/4 diagram”, Earth-Science Reviews, 109, 1-19, 2011.

Denis, B.: Etude de sols fersiallitiques désaturés du plateau de Tango (Nouvelle-Calédonie), Cahiers ORSTOM. Série Pédologie, 24, 61-76, 1988.

Dumas, P.: Méthodologie de cartographie de la sensibilité des sols à l’érosion appliquée à la région de Dumbéa à Païta-Bouloupari (Nouvelle-Calédonie), Les Cahiers d’Outre-Mer. Revue de géographie de Bordeaux, 63, 567-584, 2010.

Dumas, P., Printemps, J., Mangeas, M., and Luneau, G.: Developing erosion models for integrated coastal zone management: A case study of The New Caledonia west coast, Marine Pollution Bulletin, 61, 519-529, 2010.

Evrard, O., Laceby, J. P., Huon, S., Lefèvre, I., Sengtaheuanghoung, O., and Ribolzi, O.: Combining multiple fallout radionuclides (137Cs, 7Be, 210Pbxs) to investigate temporal sediment source dynamics in tropical, ephemeral riverine systems, J Soils Sediments, 16, 1130-1144, 10.1007/s11368-015-1316-y, 2015.

Evrard, O., Durand, R., Foucher, A., Tiecher, T., Sellier, V., Onda, Y., Lefèvre, I., Cerdan, O., and Laceby, J. P.: Using spectrocolourimetry to trace sediment source dynamics in coastal catchments draining the main Fukushima radioactive pollution plume (2011–2017), Journal of Soils and Sediments, 1-12, 2019.

Evrard, O., Chaboche, P.-A., Ramon, R., Foucher, A., and Laceby, J. P.: A global review of sediment source fingerprinting research incorporating fallout radiocesium (137Cs), Geomorphology, 107103, 2020.

Garcin, M.: Exploitation des granulats en lit vif des cours d’eau de la Grande-Terre, Nouvelle-Calédonie. BRGM/RP-58531-FR. 114 p., 90 fig., 3 tabl., Bureau des Recherches Géologiques et Minières 2010.

Garcin, M., Gastaldi, Y., and Lesimple, S.: Quantification et évolution temporelle des apports miniers dans les rivières calédoniennes. BRGM/RP-66840-FR, 44 p., 23 fig., 5, Bureau des Recherches Géologiques et Minières

2017.

Gruszowski, K., Foster, I. D., Lees, J., and Charlesworth, S.: Sediment sources and transport pathways in a rural catchment, Herefordshire, UK, Hydrological Processes, 17, 2665-2681, 2003.

Hedouin, L., Pringault, O., Metian, M., Bustamante, P., and Warnau, M.: Nickel bioaccumulation in bivalves from the New Caledonia lagoon: Seawater and food exposure, Chemosphere, 66, 1449-1457, 2007.

Highley, D., Chapman, G. R., and Bonel, K.: The economic importance of minerals to the UK, British Geological Survey, 2004.

Iltis, J.: La mine, élement de la controverse écologique dans le Pacifique Sud, L'Espace géographique, 193-205, 1992.

James, L. A.: Legacy sediment: definitions and processes of episodically produced anthropogenic sediment, Anthropocene, 2, 16-26, 2013.

Juillot, F.: – Rapport scientifique final. Programme « Dynamique des métaux de la mine au lagon ». CNRT « Nickel & son environnement ». 202 pages., 2019.

Klages, M., and Hsieh, Y.: Suspended Solids Carried by the Gallatin River of Southwestern Montana: II. Using Mineralogy for Inferring Sources 1, Journal of Environmental Quality, 4, 68-73, 1975.

Kumar, A., and Maiti, S. K.: Assessment of potentially toxic heavy metal contamination in agricultural fields, sediment, and water from an abandoned chromite-asbestos mine waste of Roro hill, Chaibasa, India, Environmental earth sciences, 74, 2617-2633, 2015.

Laceby, J. P., and Olley, J.: An examination of geochemical modelling approaches to tracing sediment sources incorporating distribution mixing and elemental correlations, Hydrol. Process., 29, 1669-1685, 10.1002/hyp.10287, 2015.

Laceby, J. P., Evrard, O., Smith, H. G., Blake, W. H., Olley, J. M., Minella, J. P. G., and Owens, P. N.: The challenges and opportunities of addressing particle size effects in sediment source fingerprinting: A review, Earth-Sci. Rev., 169, 85-103, 10.1016/j.earscirev.2017.04.009, 2017.

Le Gall, M., Evrard, O., Foucher, A., Laceby, J. P., Salvador-Blanes, S., Manière, L., Lefèvre, I., Cerdan, O., and Ayrault, S.: Investigating the temporal dynamics of suspended sediment during flood events with 7 Be and 210 Pb xs measurements in a drained lowland catchment, Scientific reports, 7, 42099, 2017.

Legout, C., Poulenard, J., Nemery, J., Navratil, O., Grangeon, T., Evrard, O., and Esteves, M.: Quantifying suspended sediment sources during runoff events in headwater catchments using spectrocolorimetry, J Soils Sediments, 13, 1478-1492, 10.1007/s11368-013-0728-9, 2013.

Mardhel, V., Iseppi, M., Regninger, P. A., and Sevin, B.: Connaissance de l'ophiolite, géophysique aéroportée et étude de la structure. Rapport scientifique final. Programme «OPHIOSTRUCT». CNRT «Nickel & son environnement», 2018.

Martínez-Carreras, N., Udelhoven, T., Krein, A., Gallart, F., Iffly, J. F., Ziebel, J., Hoffmann, L., Pfister, L., and Walling, D. E.: The use of sediment colour measured by diffuse reflectance spectrometry to determine sediment sources: application to the Attert River catchment (Luxembourg), J Hydrol, 382, 49-63, 2010.

Motha, J., Wallbrink, P., Hairsine, P., and Grayson, R.: Unsealed roads as suspended sediment sources in an agricultural catchment in south-eastern Australia, Journal of Hydrology, 286, 1-18, 2004.

Navratil, O., Evrard, O., Esteves, M., Legout, C., Ayrault, S., Némery, J., Mate-Marin, A., Ahmadi, M., Lefèvre, I., and Poirel, A.: Temporal variability of suspended sediment sources in an alpine catchment combining river/rainfall monitoring and sediment fingerprinting, Earth Surface Processes and Landforms, 37, 828-846, 2012.

Owens, P. N., and Walling, D. E.: The phosphorus content of fluvial sediment in rural and industrialized river basins, Water Res., 36, 685-701, 2002.

Pascal, N.: Ecosystèmes coralliens de Nouvelle-Calédonie. Valeur économique des services écosystémiques. Partie I: Valeur financière. IFRECOR., 2010.

Poulenard, J., Perrette, Y., Fanget, B., Quetin, P., Trevisan, D., and Dorioz, J.-M.: Infrared spectroscopy tracing of sediment sources in a small rural watershed (French Alps), Science of the Total Environment, 407, 2808-2819, 2009.

Poulenard, J., Legout, C., Nemery, J., Bramorski, J., Navratil, O., Douchin, A., Fanget, B., Perrette, Y., Evrard, O., and Esteves, M.: Tracing sediment sources during floods using Diffuse Reflectance Infrared Fourier Transform Spectrometry (DRIFTS): A case study in a highly erosive mountainous catchment (Southern French Alps), Journal of Hydrology, 414, 452-462, 2012.

Priadi, C., Ayrauk, S., Pacini, S., and Bonte, P.: Urbanization impact on metals mobility in riverine suspended sediment: role of metal oxides, International Journal of Environmental Science & Technology, 8, 1-18, 2011.

Prior, T., Daly, J., Mason, L., and Giurco, D.: Resourcing the future: Using foresight in resource governance, Geoforum, 44, 316-328, 2013.

Quantin, P., Bourdon, E., and Becquer, T.: Minéralogie et contraintes édaphiques des sols" ferritiques" dérivés de roches ultrabasiques en Nouvelle-Calédonie: relations entre constituants minéraux et disponiblité en certains éléments (Al, Fe, Si, Mg, Mn, Ni, Co, Cr, Cu, Zn, Mo) facilement solubles, 1997.

Rossel, R. V., Walvoort, D., McBratney, A., Janik, L. J., and Skjemstad, J.: Visible, near infrared, mid infrared or combined diffuse reflectance spectroscopy for simultaneous assessment of various soil properties, Geoderma, 131, 59-75, 2006.

Sellier, V., Navratil, O., Laceby, J. P., Allenbach, M., Lefèvre, I., and Evrard, O.: Investigating the use of fallout and geogenic radionuclides as potential tracing properties to quantify the sources of suspended sediment in a mining catchment in New Caledonia, South Pacific, Journal of Soils and Sediments, 1-17, 2019.

Sevin, B.: Cartographie du régolithe sur formation ultrabasique de Nouvelle-Calédonie: Localisation dans l’espace et le temps des gisements nickélifères, Nouvelle Calédonie, 2014.

Shellberg, J., Brooks, A., and Spencer, J.: Land-use change from indigenous management to cattle grazing initiates the gullying of alluvial soils in northern Australia, 19th World Congress of Soil Science: Soil Solutions for a Changing World, 2010, 1-6,

Sherriff, S. C., Franks, S. W., Rowan, J. S., Fenton, O., and Ó’hUallacháin, D.: Uncertainty-based assessment of tracer selection, tracer non-conservativeness and multiple solutions in sediment fingerprinting using synthetic and field data, J Soils Sediments, 15, 2101-2116, 10.1007/s11368-015-1123-5, 2015.

Smith, H. G., Sheridan, G. J., Lane, P. N. J., Noske, P. J., and Heijnis, H.: Changes to sediment sources following wildfire in a forested upland catchment, southeastern Australia, Hydrol. Process., 25, 2878-2889, 10.1002/hyp.8050, 2011.

Surell, A.: Étude sur les torrents des Hautes-Alpes, Carilian-Goeury, 1841.

Tiecher, T., Caner, L., Minella, J. P., and dos Santos, D. R.: Combining visible-based-color parameters and geochemical tracers to improve sediment source discrimination and apportionment, Sci Total Environ, 527-528, 135-149, 10.1016/j.scitotenv.2015.04.103, 2015.

Trescases, J. J.: Weathering and geochemical behaviour of the elements of ultramafic rocks in New Caledonia, BMRJ. Aust. Geol and Geophys., 141, 149-161, 1973.

Uber, M., Legout, C., Nord, G., Crouzet, C., Demory, F., and Poulenard, J.: Comparing alternative tracing measurements and mixing models to fingerprint suspended sediment sources in a mesoscale Mediterranean catchment, Journal of Soils and Sediments, 1-19, 2019.

Valette-Silver, N. J.: The use of sediment cores to reconstruct historical trends in contamination of estuarine and coastal sediments, Estuaries, 16, 577-588, 1993.

Varol, M.: Assessment of heavy metal contamination in sediments of the Tigris River (Turkey) using pollution indices and multivariate statistical techniques, Journal of Hazardous Materials, 195, 355-364, 2011.

Wallbrink, P., Murray, A., Olley, J., and Olive, L.: Determining sources and transit times of suspended sediment in the Murrumbidgee River, New South Wales, Australia, using fallout 137Cs and 210Pb, Water Resour Res, 34, 879-887, 1998.

Wallbrink, P. J.: Quantifying the erosion processes and land-uses which dominate fine sediment supply to Moreton Bay, Southeast Queensland, Australia, Journal of environmental radioactivity, 76, 67-80, 2004.

Walling, D., Peart, M., Oldfield, F., and Thompson, R.: Suspended sediment sources identified by magnetic measurements, Nature, 281, 110, 1979.

Yellishetty, M., Mudd, G. M., and Shukla, R.: Prediction of soil erosion from waste dumps of opencast mines and evaluation of their impacts on the environment, International Journal of Mining, Reclamation and Environment, 27, 88-102, 2013.